

Low-Rank Online Dynamic Assortment with Dual Contextual Information

Seong Jin Lee*

Will Wei Sun†

Yufeng Liu‡

Abstract

As e-commerce expands, delivering real-time personalized recommendations from vast catalogs poses a critical challenge for retail platforms. Maximizing revenue requires careful consideration of both individual customer characteristics and available item features to continuously optimize assortments over time. In this paper, we consider the dynamic assortment problem with dual contexts – user and item features. In high-dimensional scenarios, the quadratic growth of dimensions complicates computation and estimation. To tackle this challenge, we introduce a new low-rank dynamic assortment model to transform this problem into a manageable scale. Then we propose an efficient algorithm that estimates the intrinsic subspaces and utilizes the upper confidence bound approach to address the exploration-exploitation trade-off in online decision making. Theoretically, we establish a regret bound of $\tilde{O}((d_1 + d_2)r\sqrt{T})$, where d_1, d_2 represent the dimensions of the user and item features respectively, r is the rank of the parameter matrix, and T denotes the time horizon. This bound represents a substantial improvement over prior literature, achieved by leveraging the low-rank structure. Extensive simulations and an application to the Expedia hotel recommendation dataset further demonstrate the advantages of our proposed method.

Keywords— Bandit algorithm, low-rankness, online decision making, regret analysis, reinforcement learning

*Ph.D. student, Department of Statistics and Operations Research, University of North Carolina, Chapel Hill. Email: slee7@unc.edu

†Associate Professor, Daniels School of Business, Purdue University. Email: sun244@purdue.edu

‡Professor, Department of Statistics, University of Michigan, Email: yufliu@umich.edu.

1 Introduction

The assortment selection problem is a key challenge for retailers, who often face constraints on the number of items they can offer customers despite having a wide array of products. In the dynamic e-commerce environment, rich real-time information about customers and items drives the need for personalized algorithms adept at adapting to changing conditions. In online retail, the platform determines product recommendations by leveraging past assortment offerings and the users' choices on their assortment offerings. Figure 1 illustrates the contextual dynamic assortment problem: At each time, a customer arrives with user features, the platform estimates user preferences on items based on historical data and current features, selects a subset from the item catalog to present to the current user and records user choices for improving future assortment selection.

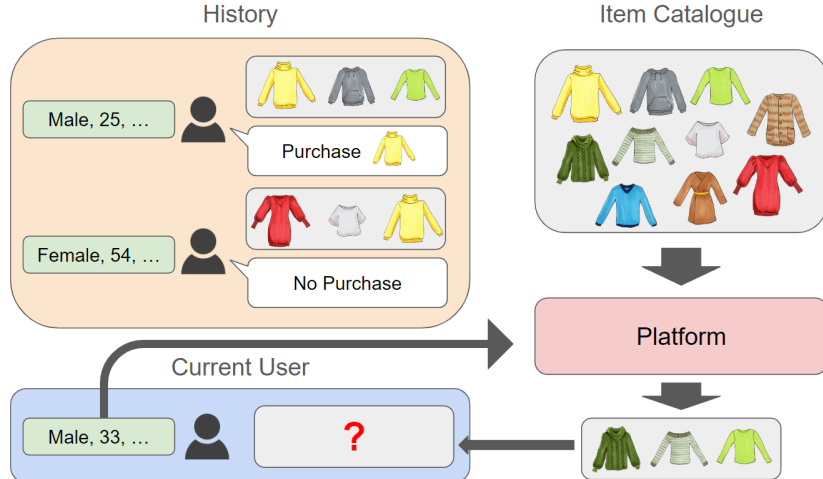


Figure 1: Illustration of the contextual dynamic assortment problem.

The primary objective of the platform is to maximize the total revenue over a time horizon T . It can adopt a ‘greedy strategy’ aimed at maximizing the revenue for each individual user by offering what is estimated as the best assortment at each time. However, due to the uncertainty of estimation, pure exploitation would lead to sub-optimal actions. To improve the accuracy of estimating these optimal assortments, the platform must delve into exploring user behaviors across various items. These two strategies, exploration for improving user preference estimation and exploitation

for revenue maximization, often do not align in online decision making problems. Reinforcement learning, an area gaining increasing attention in statistics (Chakraborty and Murphy, 2014; Zhao et al., 2015; Shi et al., 2018, 2023; Zhou et al., 2024b), provides valuable insights for navigating the delicate balance of the exploration-exploitation trade-off.

In recent years, a plethora of studies have utilized bandit and reinforcement learning algorithms (Lattimore and Szepesvari, 2020) to address the dynamic assortment problem. Some research focuses on the non-contextual scenario (Chen and Wang, 2018; Agrawal et al., 2019), while others delve into the contextual setups (Chen et al., 2020; Oh and Iyengar, 2021; Goyal and Perivier, 2022) under the multinomial logit (MNL) choice model (McFadden, 1974) to characterize user behaviors. Advances in digital retail platform infrastructure have empowered these platforms with rich data on items and users, including demographics, search histories, and purchase records. By harnessing user features, the platform can tailor personalized assortments by looking back at the choice history of users with similar user contexts. Similarly, utilizing item features allows the platform to infer item preferences by analyzing the choice history of items sharing similar item contexts, even when the item has limited inclusion in assortment history. This motivates us to study the contextual dynamic assortment problem, specifically focusing on the incorporation of “dual contextual information” involving both items and users.

In contextual dynamic assortment, a common strategy for handling dual contexts is to stack the dual features as a joint feature vector and utilize its linear form (Sumida and Zhou, 2023). Let $q_t \in \mathbb{R}^{d_1}$ be the vector representation of the feature of user t and $p_i \in \mathbb{R}^{d_2}$ be a vector representation of the feature of item i . By stacking the dual features as $x_{it} = (1, p_i^\top, q_t^\top)^\top \in \mathbb{R}^{d_1+d_2+1}$, the utility of item i for user t is represented as $v_{it} = x_{it}^\top \phi$ with vector parameter $\phi \in \mathbb{R}^{d_1+d_2+1}$; see Figure 2. However, this approach fails to capture the interaction terms between the user feature and the item feature. Consider the effect of item price on the utility of an item to a user. The effect will be different across different users, some users might be sensitive to the price, while others may be not. Similarly, the red color of an item may have a positive effect on the utility if the user prefers

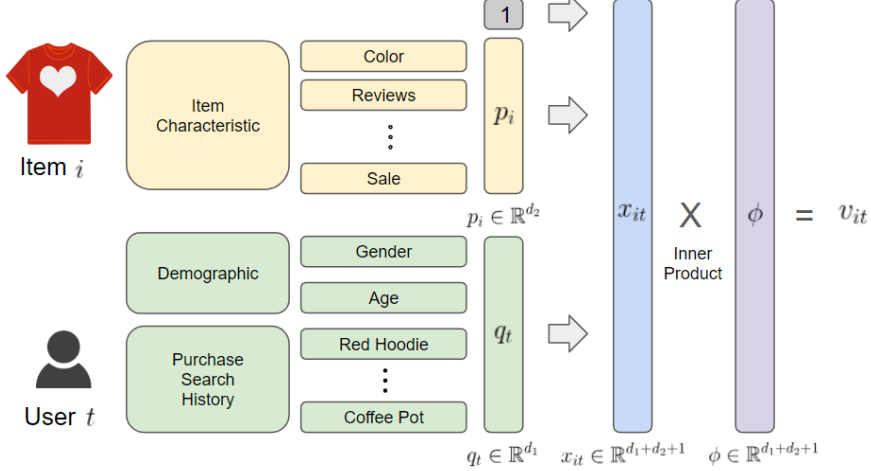


Figure 2: Stacked utility formulation of item and user features.

red items, but will have a negative effect if the user dislikes red items. The additive nature of the stack formulation cannot capture this intrinsic interaction between the two sides of features.

Another approach involves utilizing the vectorization of the combined effects of the two features as a joint feature vector, followed by the application of existing contextual dynamic assortment selection methods (Agrawal et al., 2019; Oh and Iyengar, 2021). By including the intercept and taking the outer product of the two extended features, it accounts for the intercept, main effects, and user-item interaction effects simultaneously; see Figure 3. However, in high-dimensional settings, the dimension of the outer product is $(d_1 + 1) \times (d_2 + 1)$, which scales with the product of the dimensions of the dual features, making the estimation of the effects computationally challenging.

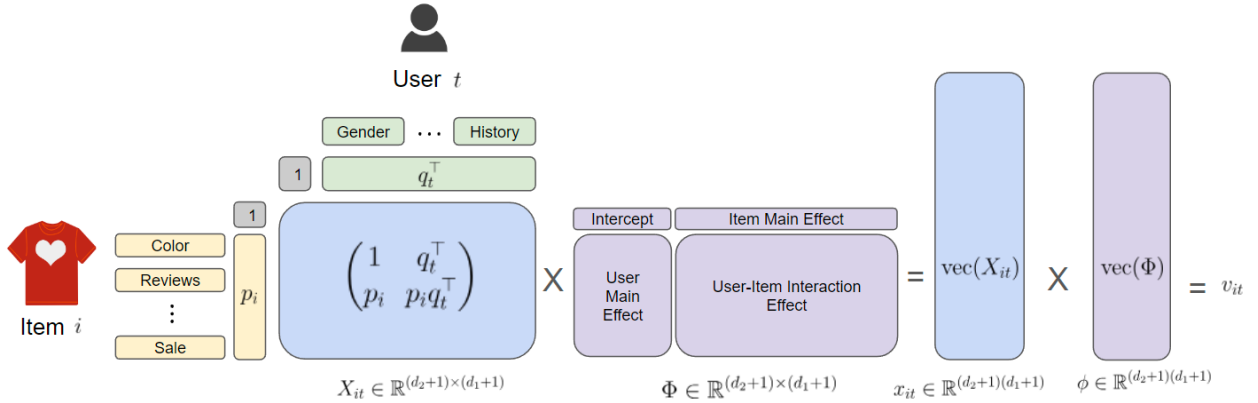


Figure 3: Vectorized utility formulation of interactions between user and item features.

In online retail, high-dimensional features can often be condensed into lower-dimensional latent factors. For instance, user traits like buying power can be inferred as a combination of income, education level, and past purchase behaviors. This buying power directly influences item utility, interacting with features such as price. Similarly, color preferences can be estimated from demographic data and previous red item purchases. Despite a user’s extensive purchase history spanning numerous items, its impact on red item utility can be simplified into a scalar value. Likewise, an item’s characteristics can be projected onto a reduced-dimensional latent space. Consequently, interaction effects between these dual contexts can be characterized by a smaller set of latent factors, as depicted in Figure 4. By addressing the dual contextual problem within a low-rank structure,

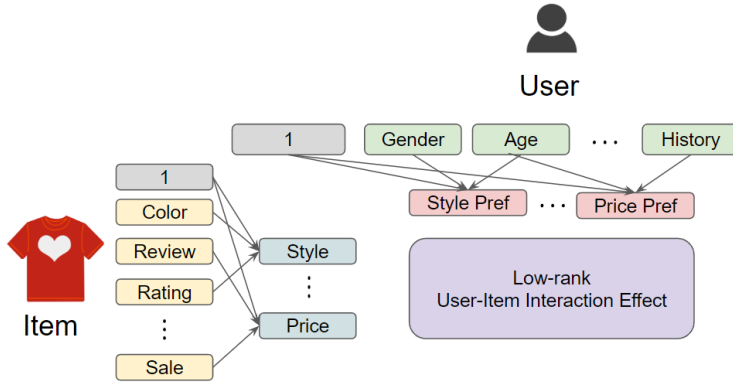


Figure 4: Illustration of low-rank user-item interaction effect.

while retaining the impact of the features on the user preferences for items, we effectively reduce the dimension of the target parameter. This not only enhances computational efficiency but also reduces the cumulative estimation error across parameter components.

Inspired by this observation, in this paper we adopt the bilinear form $v = p^\top \Phi q$ with a low-rank matrix parameter Φ to represent utilities. This form offers flexibility, accommodating both stacking and vectorization approaches of incorporating dual features. The stack approach can be interpreted as the bilinear form with intercepts and a rank-2 parameter matrix while the vectorization approach can be interpreted as the scenario with full rank. Moreover, we can reduce the computational complexity by imposing a low-rank structure on Φ , reducing the dimension of the parameter from $d_1 d_2$ to $(d_1 + d_2)r$, where $r (\ll \min\{d_1, d_2\})$ is the rank of the parameter matrix. Low-rank models

have garnered growing interest in statistics (Jain et al., 2013; Xia and Yuan, 2021; Xia et al., 2022; Ma et al., 2024) with diverse scientific and business applications (Bell and Koren, 2007; Koren et al., 2009; Udell and Townsend, 2019; Zhen and Wang, 2024; Zhou et al., 2024a). Following this trend, our paper considers a new Low-rank Online Assortment with Dual-contexts (LOAD) problem.

To solve the LOAD problem, we propose an Explore-Low-rank-Subspace-then-Apply-UCB (ELSA-UCB) algorithm which consists of two main stages: subspace exploration and the application of Upper Confidence Bound (UCB). The major computational bottleneck arises from estimating the entire preference parameter matrix. To overcome this challenge, we project the features and parameters to a low-dimensional subspace. In the first stage, we leverage the inherent low-rank structure to estimate the low-dimensional subspace of the matrix parameter. To accomplish this, we explore the space by employing random assortments and then solve the rank-constrained likelihood maximization problem to estimate the subspace. Given the non-convex nature of the rank-constrained optimization problem, we adopt the alternating gradient descent algorithm based on the Burer-Monteiro formulation (Burer and Monteiro, 2003; Zheng and Lafferty, 2016; Chi et al., 2019) to estimate the parameter matrix. Subsequently, we perform singular value decomposition (SVD) on the estimated matrix to derive the intrinsic subspace. Utilizing the estimated subspace, we rotate the features and parameters in accordance with the subspace, then truncate negligible terms to effectively reduce the problem’s dimensionality. In the second stage, we employ the UCB-based strategy on the reduced dimension based on careful construction of the confidence bounds in this space. UCB uses an “optimism in the face of uncertainty” idea that addresses the exploration-exploitation trade-off by selecting the best action based on the “optimistic reward”, the upper confidence bound of the estimated reward (Auer, 2002; Lattimore and Szepesvári, 2020). Contrary to the unbiased model in the original parameter space, the preference model within the reduced space is inherently biased with respect to the estimated subspaces. To handle this, we introduce a novel tool that provides a confidence bound for the expected reward on the reduced space, by correcting this bias. Implementing the UCB-based policy in this reduced space reduces the param-

eter dimension from $d_1 \times d_2$ to $r(d_1 + d_2) - r^2$. This reduction markedly improves computational efficiency, reduces estimation error, and enhances the algorithm performance. In practice, the rank of the underlying parameter matrix is often unknown. To address this issue, we propose ELSA-GIC, incorporating the rank selection procedure using Generalized Information Criterion (GIC) (Konishi and Kitagawa, 1996; Fan and Tang, 2013) into ELSA-UCB. We also prove rank selection consistency of ELSA-GIC in the LOAD problem.

To assess the theoretical performance of our proposed algorithm, we study the cumulative regrets of our policy. The regret is defined as the difference between the optimal reward from the oracle possessing complete knowledge of environmental parameters and the reward obtained from a given policy. In theory, we establish an $\tilde{O}((d_1 + d_2)r\sqrt{T})$ regret upper bound for our proposed ELSA-UCB policy (Theorem 1). Notably, in low-rank setups with $r \ll \min\{d_1, d_2\}$, our regret bound is much improved from $\tilde{O}(d_1 d_2 \sqrt{T})$ regret bounds achieved by existing methods (Chen et al., 2020; Oh and Iyengar, 2021) that vectorize the outer product of the dual features.

The regret analysis for our policy presents several challenges. Firstly, in the dual-contextual environment, the distribution of joint features depends on the assortment selection, violating the i.i.d. feature assumption in existing dynamic assortment selection literature (Chen et al., 2020; Oh and Iyengar, 2021). To accommodate this, we impose minimal assumptions on the item features (Assumption 2) to ensure the identifiability of parameters. Secondly, the non-convex nature of the low-rank optimization problem precludes us from leveraging classical convex optimization theories. While Jun et al. (2019); Kang et al. (2022) studied generalized linear bandits with low-rank structure, their analysis tools are not applicable to our LOAD problem due to the unique combinatorial structure in the dynamic assortment selection. Thus, we establish novel estimation bounds specifically tailored for the rank-constrained optimization problem on assortment scenarios.

Finally, we present numerical results to demonstrate the effectiveness of our algorithm. Initially, we evaluate the ELSA-GIC policy's performance on synthetic data, exploring various scenarios including changing ranks, feature dimensions, number of items, and assortment capacity. We

compare cumulative regret over different time horizons with two variants of the UCB-MNL policy (Oh and Iyengar, 2021): Stacked UCB-MNL and Vectorized UCB-MNL. Our analysis consistently shows that ELSA-GIC outperforms both methods across all scenarios, with the performance gap widening in scenarios with lower ranks and higher dimensions. We also show the robust performance of ELSA-GIC under model mis-specification. Additionally, we conduct real data analysis on the Expedia dataset to optimize hotel recommendations. Our findings demonstrate that the parameter matrix exhibits a low-dimensional structure, and our method effectively leverages this to achieve improved performance, highlighting its practical usefulness.

1.1 Related Work

Our work is closely related to recent studies on contextual dynamic assortment selection and low-rank bandits. Additional relevant literature is provided in Section S.1 of the supplement.

• Contextual Dynamic Assortment Selection

Inspired by the foundational work by Caro and Gallien (2007), numerous studies have explored the dynamic assortment problem under the MNL bandit model. Various policies, including Explore-Then-Commit (Rusmevichtong et al., 2010; Sauré and Zeevi, 2013), Thompson Sampling (Agrawal et al., 2017) and UCB (Agrawal et al., 2019) have been proposed to address the balance between exploration and exploitation in the MNL bandit model. Other studies consider various scenarios such as robustness against outliers (Chen et al., 2023), multi-stage choices (Xu and Wang, 2023) or extension to different choice models (Aouad et al., 2023). Contextual dynamic assortment considers various facets, including item-specific features (Wang et al., 2019), time-varying item features (Chen et al., 2020), user types (Kallus and Udell, 2020), item features (Shao et al., 2022), or features associated with user-item pairs (Oh and Iyengar, 2021; Goyal and Perivier, 2022). These features are utilized in modeling utilities for the MNL bandit model. However, while existing algorithms address single-context scenarios, focusing solely on users or items, they lack the capability

to estimate interactions between dual contexts. Although algorithms designed for joint features on user-item pairs could be applied to the dual contextual setup by interpreting the vectorization of the outer product of dual features, this approach inevitably encounters large computational burdens and fails to capture the low-rank structure of the parameter matrix in our LOAD problem. Our proposed method aims to fill this gap.

- **Low-Rank Bandits**

The dynamic environment involving high-dimensional covariates has also been a vibrant area of research. Based on a rich background of statistical tools for high dimensional problems (Wainwright, 2019), numerous studies addressed the ‘curse of dimensionality’ in high-dimensional bandits. These studies often assume sparsity in the parameter vector and employ the LASSO-based approach (Abbasi-Yadkori et al., 2012; Kim and Paik, 2019) or presume the low-rank structure within the parameter matrix (Jun et al., 2019; Kang et al., 2022; Cai et al., 2023; Zhou et al., 2024a). While certain studies have utilized the LASSO-based approach to address the sparse dynamic assortment problem (Wang et al., 2019; Shao et al., 2022), there has been comparatively less emphasis on leveraging the low-rank structure in the dynamic assortment. Recently, Cai et al. (2023) approached the dynamic assortment problem by modeling rewards as a bilinear form of action and context. However, they did not consider any user choice model and overlooked the inherent structure between assortment sets. Because of this, their algorithms and analysis tools are not applicable to our problem. To the best of our knowledge, our approach is the first one to incorporate the low-rank structure in the dynamic assortment selection with dual contexts.

1.2 Notations

Let $[n]$ denote the set $\{1, 2, \dots, n\}$. The Frobenius norm of a matrix is denoted by $\|\cdot\|_F$, and the matrix-induced norm $\|v\|_W = \sqrt{v^\top W v}$ is denoted by $\|\cdot\|_W$. The ball induced by the Frobenius norm, centered at Θ_0 with radius r is denoted by $\mathcal{B}(\Theta_0, r) := \{\Theta : \|\Theta - \Theta_0\|_F \leq r\}$. For a vector

$v, (v)_i$ represents its i -th component. We write $\Sigma_1 \succ \Sigma_2$ if $\Sigma_1 - \Sigma_2$ is positive definite. Denote the Kronecker product of two matrices by \otimes . We use the notation $\tilde{O}(a_n)$ to denote that the quantity is bounded by a_n up to logarithmic factors.

2 Problem Formulation

In this section, we introduce the mathematical formulation of the LOAD problem. At time t , a user with feature vector $q_t \in \mathbb{R}^{d_1}$ arrives at the platform. Assume there are N products, each with item feature vector $p_i \in \mathbb{R}^{d_2}$ for $i \in [N] = \{1, \dots, N\}$. The platform offers an assortment S_t of size at most K from the catalog $[N]$. In other words, $S_t \subset [N]$ and $|S_t| \leq K$. When the user is provided with an assortment, the user either chooses one of the items in the assortment or chooses not to purchase at all. To quantify this user choice, let $y_{it} \in \{0, 1\}$ represent whether user t chooses item i , for $i \in [N]$ and $t \geq 1$. In addition, denote $y_{0t} = 1$ as the indicator that user t does not choose any item at all. Let $i_t \in S_t$ be the item that user t chooses (0 if no purchase). Note that for at each user t , $y_{i_t,t} = 1$ and the remaining is $y_{jt} = 0$ for $j \in S_t \cup \{0\} \setminus \{i_t\}$, i.e., $\sum_{i \in S_t \cup \{0\}} y_{it} = 1$. Denote $\mathbf{y}_t = (y_{1t}, \dots, y_{Nt})^\top \in \{0, 1\}^N$ as the choice vector of user t .

In assortment selection, a widely adopted choice model is the multinomial logit (MNL) model (McFadden, 1974; Rusmevichientong et al., 2010; Agrawal et al., 2019). Suppose the utility of item i to user t is given as a random variable $X_{it} = v_{it} + \epsilon_{it}$, where v_{it} is the expected utility and ϵ_{it} is a mean-zero error term. Assume $v_{0t} = 0$ for identifiability. The MNL model assumes that the probability of user t choosing item i is given as

$$p_t(i) := \mathbb{P}(y_{it} = 1) = \frac{\exp(v_{it})}{1 + \sum_{j \in S_t} \exp(v_{jt})}, \quad i \in S_t,$$

and the probability of no purchase is given as $1/(1 + \sum_{j \in S_t} \exp(v_{jt}))$. In this paper, we model the utility v_{it} as a low-rank bilinear form of the dual contexts with

$$v_{it} = p_i^\top \Phi^* q_t,$$

where $\Phi^* \in \mathbb{R}^{d_2 \times d_1}$ is a rank- r matrix, illustrated in Figure 4, with singular values $\sigma_1 \geq \dots \geq \sigma_r > 0$.

After the user's purchasing decision under the MNL model, the platform earns revenue from the selected item (or zero if no purchase is made). Let r_i denote the revenue that the platform achieves when item i is sold. Given an assortment S , the revenue that the platform achieves from user t is $\sum_{i \in S} r_i y_{it}$, and the expected revenue of the platform for user t is

$$R_t(S, \Phi^*) = \mathbb{E} \left[\sum_{i \in S} r_i \cdot y_{it} \right] = \sum_{i \in S} r_i p_t(i|S, \Phi^*).$$

The platform aims to choose the personalized assortment for each user t at time t to maximize the cumulative expected revenue gained from all users. Note that the possible assortment set with constraint K , i.e., $\mathcal{S} = \{S \subset [N] : |S| \leq K\}$ is finite. Therefore, when Φ^* is known in hindsight, there exists an optimal assortment S_t^* for user t that maximizes the expected revenue since we can calculate the expected utility for every $S \in \mathcal{S}$. Denote the optimal assortment at time t as

$$S_t^* = \arg \max_{S \in \mathcal{S}} R_t(S, \Phi^*).$$

However, in practice, the true parameter Φ^* is not known to the platform. Instead, the platform chooses the assortment for each user t based on some policy. To evaluate the performance of a policy, we define regret as the difference in expected revenue between the optimal assortment and the chosen assortment from the given policy. In other words, if we choose assortments S_t for each user t , the total cumulative regret over time horizon T is defined as

$$\mathcal{R}_T = \mathbb{E} \left[\sum_{t=1}^T (R_t(S_t^*, \Phi^*) - R_t(S_t, \Phi^*)) \right].$$

Note that maximizing the cumulative revenue is equivalent to minimizing the cumulative regret. At time t , given the current user context q_t and historical data, including past assortments S_1, S_2, \dots, S_{t-1} presented to users $1, 2, \dots, t-1$ with respective features q_1, q_2, \dots, q_{t-1} , and the corresponding feedback $\mathbf{y}_1, \mathbf{y}_2, \dots, \mathbf{y}_{t-1}$, the platform needs to determine the assortment S_t for the user t so that the cumulative regret could be small.

3 Algorithm

In this section, we propose our Explore-Low-rank-Subspace-then-Apply-UCB (ELSA-UCB) method to address the LOAD problem defined in the previous section. The algorithm is mainly composed of two stages. The first stage is the exploration stage with random assortments which aims to estimate the low-dimensional subspace of the matrix parameter Φ^* . Using the estimated subspace, we rotate the parameter and feature space and truncate the negligible dimensions. In the second stage, we use a UCB-based approach on the estimated subspace to select the assortment with the highest possible reward.

3.1 Estimation of Subspace

The first stage of the algorithm aims to acquire estimations of low-rank subspaces. Let $\Phi^* = U^* D^* (V^*)^\top$ be the singular value decomposition of Φ^* , where $U^* \in \mathbb{R}^{d_2 \times d_2}$, $V^* \in \mathbb{R}^{d_1 \times d_1}$ are square orthonormal matrices and $D^* \in \mathbb{R}^{d_2 \times d_1}$ is a diagonal matrix with singular values as its diagonal components. Let $u_{(j)}^*$ be the j -th column of U^* and $v_{(j)}^*$ be the j -th column of V^* . Consider dual contexts $p \in \mathbb{R}^{d_2}$ and $q \in \mathbb{R}^{d_1}$. The bilinear form of p and q with respect to Φ^* can be rewritten as

$$p^\top \Phi^* q = ((U^*)^\top p)^\top D^* ((V^*)^\top q) = \sum_{j=1}^r d_j p'_j q'_j,$$

where $p'_j = (u_{(j)}^*)^\top p$ and $q'_j = (v_{(j)}^*)^\top q$ are rotations of p and q each with respect to orthonormal basis U^* and V^* . Thus, the first r columns of U and V each capture the r latent features originating from dual contexts, which affect user preferences toward items. Consequently, by estimating the subspace of the matrix Φ^* via estimating U^* and V^* , the platform effectively extracts the low-dimensional latent features, maintaining the representational capability of the original features.

For estimation of the subspace, we start with random assortments offered to the first T_0 users to achieve an initial estimate of Φ^* . Consider the rank-constrained likelihood maximization problem:

$$\min_{\Phi \in \mathbb{R}^{d_2 \times d_1}, \text{rank}(\Phi) \leq r} \mathcal{L}_n(\Phi), \quad (1)$$

where $\mathcal{L}_n(\Phi)$ is the negative log-likelihood of the MNL choice model with n samples, expressed as

$$\mathcal{L}_n(\Phi) = -\frac{1}{n} \sum_{t=1}^n \left[\sum_{i \in S_t} y_{it} p_i^\top \Phi q_t - \log \left(1 + \sum_{j \in S_t} \exp(p_j^\top \Phi q_t) \right) \right].$$

To solve this rank-constrained optimization, we use the Burer-Monteiro formulation (Burer and Monteiro, 2003) to optimize over $U \in \mathbb{R}^{d_2 \times r}$ and $V \in \mathbb{R}^{d_1 \times r}$, where $\Phi = UV^\top$. We add a regularization term to enforce identifiability (Zheng and Lafferty, 2016). This leads to our final optimization problem:

$$\min_{U \in \mathbb{R}^{d_2 \times r}, V \in \mathbb{R}^{d_1 \times r}} \left(\tilde{\mathcal{L}}_n(U, V) := \mathcal{L}_n(UV^\top) + \frac{1}{8} \|U^\top U - V^\top V\|_F^2 \right). \quad (2)$$

This non-convex optimization can be solved effectively via an alternating factored gradient descent (FGD). FGD simply applies gradient descent on each factor,

$$U \leftarrow U - \eta \cdot \nabla_U \tilde{\mathcal{L}}_n(U, V), \quad V \leftarrow V - \eta \cdot \nabla_V \tilde{\mathcal{L}}_n(U, V),$$

where η is the learning rate, ∇_U, ∇_V are gradients with respect to each component when other parameters are fixed. Applying these gradient descent steps alternatively, the estimated parameters are known to converge to the true parameters given conditions on the initial estimate (Zheng and Lafferty, 2016; Zhang et al., 2023). Details of FGD are given in Algorithm 1.

Algorithm 1 FGD - Factored Gradient Descent

Input: Gradients of the loss function $\nabla_U \tilde{\mathcal{L}}$ and $\nabla_V \tilde{\mathcal{L}}$, initial estimate Φ_0 and step size η .
Initialization: SVD $\Phi_0 = U_0 D_0 V_0^\top$ and initialize $U^{(0)} = U_0 D_0^{1/2}$ and $V^{(0)} = V_0 D_0^{1/2}$.

```

1: for  $k = 1, \dots$ , do
2:   Update  $U^{(k+1)} = U^{(k)} - \eta \nabla_U \tilde{\mathcal{L}}|_{U=U^{(k)}, V=V^{(k)}}$ .
3:   Update  $V^{(k+1)} = V^{(k)} - \eta \nabla_V \tilde{\mathcal{L}}|_{U=U^{(k+1)}, V=V^{(k)}}$ .
4:   Repeat until objective function converges.
5: end for
return  $\hat{\Phi} = U^{(k)}(V^{(k)})^\top$ .
```

For the initialization of FGD, we use the unconstrained maximum likelihood estimator (MLE) of Φ^* . As the likelihood function is convex, we can apply a convex optimization algorithm such as

the gradient-based algorithm or L-BFGS (Liu and Nocedal, 1989) to calculate the initialization.

With the estimate $\hat{\Phi}$ from Algorithm 1, we obtain the estimated subspaces \hat{U} and \hat{V} via SVD, $\hat{\Phi} = \hat{U}\hat{D}\hat{V}^\top$. Next, we rotate the original subspace with respect to the estimated subspace. We partition $U^*, V^*, \hat{U}, \hat{V}$ into $(U_1^*, U_2^*), (V_1^*, V_2^*), (\hat{U}_1, \hat{U}_2), (\hat{V}_1, \hat{V}_2)$, where $(\cdot)_1$ denotes the first r columns and $(\cdot)_2$ denotes the remaining columns of a matrix. Define

$$\begin{aligned}\Theta^* &:= \hat{U}^\top \Phi^* \hat{V} = (\hat{U}_1, \hat{U}_2)^\top U_1^* D_{11} (V_1^*)^\top (\hat{V}_1, \hat{V}_2) \\ &= \begin{pmatrix} (\hat{U}_1^\top U_1^*) D_{11}^* (\hat{V}_1^\top V_1^*)^\top & (\hat{U}_1^\top U_1^*) D_{11}^* (\hat{V}_2^\top V_1^*)^\top \\ (\hat{U}_2^\top U_1^*) D_{11}^* (\hat{V}_1^\top V_1^*)^\top & (\hat{U}_2^\top U_1^*) D_{11}^* (\hat{V}_2^\top V_1^*)^\top \end{pmatrix}.\end{aligned}$$

We adopt the “subtraction method” prevalent in the low-rank matrix bandit (Kveton et al., 2017; Jun et al., 2019; Kang et al., 2022). Note that $\hat{U}_2^\top U_1^*$ and $\hat{V}_2^\top V_1^*$ are expected to be small, assuming that \hat{U}, \hat{V} are good estimations of U^*, V^* . Thus its product $(\hat{U}_2^\top U_1^*)(\hat{V}_2^\top V_1^*)^\top$ is expected to be negligible. To utilize this structure, we introduce the notation of “truncation-vectorization” of matrices. Consider $\Theta \in \mathbb{R}^{d_2 \times d_1}$ with block-sub-matrices $\Theta_{11} \in \mathbb{R}^{r \times r}$, $\Theta_{12} \in \mathbb{R}^{r \times (d_1-r)}$, $\Theta_{21} \in \mathbb{R}^{(d_2-r) \times r}$, $\Theta_{22} \in \mathbb{R}^{(d_2-r) \times (d_1-r)}$. Define “truncation-vectorization” of Θ as

$$\theta_{rtv} := (\text{vec}(\Theta_{11})^\top, \text{vec}(\Theta_{12})^\top, \text{vec}(\Theta_{21})^\top)^\top \in \mathbb{R}^{(d_1+d_2)r-r^2}, \quad (3)$$

where “ rtv ” is an abbreviation of “rotation-truncation-vectorization” to represent that the original matrix Φ^* has been rotated with respect to \hat{U} and \hat{V} , then truncated and vectorized.

Note that $\Theta_{22}^* = (\hat{U}_2^\top U_1^*) D_{11}^* (\hat{V}_2^\top V_1^*)^\top$ is expected to be negligible, so we only need to focus on the estimation of θ_{rtv}^* , the truncation-vectorization of Θ^* . The computational advantage of this is that the dimension of the parameter is now reduced from $d_2 d_1$ of Θ^* to $r(d_1 + d_2) - r^2$ of θ_{rtv}^* . In the rotated space, the user utility of an item is expressed as

$$v_{it} = p_i^\top \Phi^* q_t = (\hat{U}^\top p_i)^\top \Theta^* (\hat{V}^\top q_t) = \langle (\hat{U}^\top p_i)(\hat{V}^\top q_t)^\top, \Theta^* \rangle.$$

Denote $X_{it} = (\hat{U}^\top p_i)(\hat{V}^\top q_t)^\top$ and define the truncation-vectorization of X_{it} as $x_{it,rtv}$. Then

$$v_{it} = \langle X_{it}, \Theta^* \rangle = \langle x_{it,rtv}, \theta_{rtv} \rangle + \langle (X_{it})_{22}, \Theta_{22}^* \rangle \approx \langle x_{it,rtv}, \theta_{rtv} \rangle,$$

as $\Theta_{22}^* \approx 0$. Hence we can represent our original dual features as $x_{it,rtv}$ and focus on the estimation of low-dimensional parameter θ_{rtv} for our dynamic assortment selection policy.

When the rank r of the parameter matrix is unknown, we can estimate the rank using Generalized Information Criterion (GIC). GIC (Konishi and Kitagawa, 1996; Fan and Tang, 2013; Morimoto et al., 2024; Park et al., 2024) is a generalization of information criteria including Bayesian Information Criterion (BIC) and Akaike Information Criterion (AIC) (Akaike, 1987), and is widely used in the high-dimensional estimation problems to select hyper parameters to avoid over-fitting.

Adapting to our setting, we utilize the GIC in the following form:

$$GIC(r) := \mathcal{L}_n(\hat{\Phi}_r) + a_n \cdot (d_1 + d_2 - r) \cdot r, \quad (4)$$

which penalizes the number of free parameters under the low-rank assumption. We show that the selection of r is theoretically consistent with proper selection of a_n (Proposition 2 in the Appendix) and demonstrate the accuracy of rank selection with $a_n = \log(n)/n$ in our numerical results (Figure 5). We provide details of incorporating GIC to ELSA-UCB in Appendix Section S.5.2.

3.2 UCB-based Stage

The second stage of the algorithm employs the UCB approach on θ_{rtv}^* . UCB algorithm, also known as “optimism in the face of uncertainty” (Lattimore and Szepesvári, 2020), operates based on the principle that the decision-maker should select the assortment with the highest “optimistic reward”, or the upper confidence bound of the estimated reward. Even if an assortment has a low estimated expected reward, when it has a high upper confidence bound due to large uncertainty, the algorithm can still favor that assortment. This approach inherently strikes a balance between exploiting the estimated reward and exploring assortments with higher uncertainty. As the algo-

rithm is encouraged to further explore assortments with greater uncertainty, the confidence bounds gradually tighten, converging towards the true expected reward.

To adopt the UCB approach, we formulate the optimistic utility of item i to user t as

$$z_{it} = x_{it,rtv}^\top \hat{\theta}_{t,rtv} + \beta_{it}. \quad (5)$$

The first term $x_{it,rtv}^\top \hat{\theta}_{t,rtv}$ is the estimate for utility of the item i for user t , and the latter term β_{it} quantifies the uncertainty of the utility. For β_{it} , it can be calculated as $\beta_{it} = \alpha_t \cdot \|x_{it,rtv}\|_{W_t^{-1}}$, where the selection of α_t is based on the confidence bound of $\hat{\theta}_{t,rtv}$ established in Lemma 1 of Section 4 and $W_t = \sum_{s=1}^t \sum_{i \in S_s} x_{is,rtv} x_{is,rtv}^\top$. Then we choose the optimal assortment that maximizes the revenue under the optimistic utilities. In other words, we offer the assortment $S_t = \arg \max_{S \in \mathcal{S}} \tilde{R}_t(S)$, where

$$\tilde{R}_t(S) := \sum_{i \in S} r_i \cdot \frac{\exp(z_{it})}{1 + \sum_{j \in S} \exp(z_{it})}.$$

After obtaining the optimistic utilities, this problem can be solved via the StaticMNL policy introduced for the static assortment problem (Rusmevichientong et al., 2010).

During the construction of confidence bounds for the optimistic reward, the algorithm simultaneously updates the estimate $\hat{\theta}_{t,rtv}$. Distinct from the rank-constrained MLE in the first stage, in the UCB-based stage, we solve a new estimator for the updated parameter θ_{rtv}^* . Since the parameter dimensionality has reduced from $d_1 \times d_2$ in the first stage to $(d_1 + d_2)r - r^2$ in this UCB-stage, we can calculate the MLE directly on the reduced space to obtain $\hat{\theta}_{n,rtv} = \arg \min \mathcal{L}_{n,rtv}(\theta_{rtv})$, where $\mathcal{L}_{n,rtv}$ is the negative log-likelihood in the reduced space with

$$\mathcal{L}_{n,rtv}(\theta_{rtv}) = \frac{1}{n} \sum_{t=1}^n \left[\sum_{i \in S_t} y_{it} x_{it,rtv}^\top \theta_{rtv} - \log \left(1 + \sum_{j \in S_t} \exp(x_{it,rtv}^\top \theta_{rtv}) \right) \right]. \quad (6)$$

It is crucial to note that this optimization problem is simpler than the rank-constrained MLE in (1) or (2), since this optimization is unconstrained and many existing convex optimization techniques can be employed to solve (6).

Remark 1 (Cold-start and Long-tail Issues). *A common challenge in recommender systems is the*

Algorithm 2 ELSA-UCB - Explore Low-dimensional Subspace then Apply UCB

Input: Assortment capacity K , rank of parameter matrix r , learning rate η , initial parameter estimate Φ_0 and exploration length T_0 .

- 1: Observe item feature vectors $p_i, i \in [N]$.
- 2: **for** $t = 1, \dots, T_0$, **do**
- 3: Observe the current user feature vector q_t .
- 4: Randomly select a size K assortment $S_t \in \mathcal{S}$ and observe user choice \mathbf{y}_t .
- 5: **end for**
- 6: Estimate the low-rank matrix $\hat{\Phi} = \arg \max_{rk(\Phi)=r} \mathcal{L}_n(\Phi)$ using Algorithm 1.
- 7: Estimate the subspace using SVD $\hat{\Phi} = \hat{U} \hat{D} \hat{V}^\top$.
- 8: Initialize $\hat{\theta}_{t,rtv} \in \mathbb{R}^k$ as the truncated vectorization of \hat{D} as in (3).
- 9: Rotate the item features $p'_i = \hat{U}^\top p_i$ for $i \in [N]$.
- 10: **for** $t = T_0 + 1, \dots, T$, **do**
- 11: Observe user feature vector q_t
- 12: Rotate the user feature $q'_t = \hat{V}^\top q_t$.
- 13: Compute $x_{it,rtv}$, the truncated vectorization of $p'_i(q'_t)^\top$ as in (3).
- 14: Compute $z_{it} = x_{it,rtv}^\top \hat{\theta}_{t,rtv} + \beta_{it}$ as in (5).
- 15: Select $S_t = \arg \max_S \hat{R}_t(S)$ via StaticMNL and observe choice \mathbf{y}_t .
- 16: Update the MLE $\hat{\theta}_{t,rtv}$ by solving (6).
- 17: **end for**

cold-start problem (Schein et al., 2002; Lika et al., 2014), where either new users or new items arrive with limited or no interaction history. Our framework addresses these scenarios through its contextual and low-rank structure. Each arriving user is represented by a feature vector, so the model does not depend on repeat arrivals. Similarly, when a new item is introduced, its feature vector p_i can be directly incorporated into the bilinear utility model $p_i^\top \Theta^ q_t$, enabling preference estimation and uncertainty quantification without requiring past interaction data. This ensures robustness in environments with dynamically evolving user and item sets.*

For long-tail items that may be chosen infrequently, the bilinear low-rank formulation helps mitigate data sparsity by sharing statistical strength across items and users. This allows utilities to be estimated reliably even when direct observations of a particular item are limited. Nonetheless, in cases where item or user features are partially unobserved, imputations based on historical data or clustering methods can be employed, though such procedures may introduce bias. Additional

strategies, such as incorporating richer content-based features or adopting active exploration targeted at under-represented items, may further improve performance, and we view these extensions as promising directions for future research.

4 Theory

In this section, we first state and discuss the feasibility of the required assumptions (Section 4.1). Next, we derive the estimation error bound on our rank-constrained maximum likelihood estimation for the LOAD problem (Proposition 1), and use this result to establish a confidence bound on the parameter in the reduced space (Lemma 1). Finally we establish an upper bound on the regret of our ELSA-UCB policy (Theorem 1).

4.1 Assumptions

First, we impose conditions on the distribution of the feature vectors.

Assumption 1 (Distribution of user features). *Each user feature q_t is i.i.d. from an unknown distribution, where $\|q_t\|_2 \leq S_q$ for some constant S_q and $\mathbb{E}[q_t q_t^\top] = \Sigma_q$ with positive definite Σ_q . Moreover, $\Sigma_q^{-1/2} q_t$ is σ -sub-Gaussian and its ℓ_2 norm bounded by some constant S_v .*

The boundness of feature vectors is common in contextual bandit and assortment problems (Li et al., 2017; Oh and Iyengar, 2021), and the invertibility of the second moment ensures that the distribution of user features is sufficient to estimate the related parameters. In addition, note that we only require the i.i.d. condition on the user features, not on the joint user and item features as in the existing dynamic assortment literature (Oh and Iyengar, 2021; Chen et al., 2020).

Assumption 2 (Design of item features). *The item features satisfy $\|p_i\|_2 \leq S_p$ for some constant S_p and assume $\Sigma_p := \frac{1}{N} \sum_{i=1}^N p_i p_i^\top$ is positive definite.*

We assume that item features are also bounded with a positive definite second moment. Note that the positive definite condition is needed to guarantee the identifiability of the matrix parameter

Φ^* , and can be verified in practice since p_i 's are given in advance. Next, we impose a standard assumption in contextual MNL problems (Oh and Iyengar, 2021), which is a slight modification of the assumption on the link function in generalized linear contextual bandits (Li et al., 2017).

Assumption 3. *There exists a constant $\kappa > 0$ such that*

$$\min_{\|\Phi - \Phi^*\|_F^2 \leq 1} p_t(i|S, \Phi) p_t(0|S, \Phi) \geq \kappa,$$

for every $S \in \mathcal{S}$, $i \in S$ and $t \in [T]$, where $p_t(i|S, \Phi)$ is the probability of selecting item i for user t under the true parameter Φ and assortment S .

This assumption ensures that the choice probabilities under the MNL model are “well-behaved” around the true parameter Φ^* . Intuitively, this assumption prevents degeneracy in the choice probabilities. That is, it avoids situations where one item dominates the entire choice set (i.e., is almost always chosen), or where the no-purchase probability becomes negligible or overwhelming. Such extreme cases would make the model highly sensitive to noise and impede reliable estimation of user preferences. In MNL-bandit models, analogous assumptions have been used in prior work, including Cheung and Simchi-Levi (2017), Chen et al. (2020), and Oh and Iyengar (2021).

4.2 Main Results

First we establish an estimation error bound on our rank-constrained maximum likelihood estimation for the LOAD problem.

Proposition 1 (Accuracy of Low-Rank Estimation). *Suppose Assumptions 1, 2 and 3 hold. Further assume we have an initial estimate $\Phi_0 \in \mathbb{R}^{d_2 \times d_1}$ such that $\|\Phi_0 - \Phi^*\|_F \leq c_2 \sqrt{\sigma_r}$ for some constant c_2 , where σ_r is r -th largest singular value of Φ^* . Let $\hat{\Phi}$ be the rank-constrained estimator using Algorithm 1 with initial estimate Φ_0 . If the exploration length T_0 satisfies*

$$T_0 \geq 4\sigma^2(C_1\sqrt{d_1 d_2} + C_2\sqrt{\log(1/\delta)})^2 + \frac{2B}{\lambda_{\min}(\Sigma)K},$$

for some constants C_1, C_2 and any $\delta \in (0, 1)$, $B > 0$, where $\Sigma = \Sigma_q \otimes \Sigma_p$, then

$$\|\hat{\Phi} - \Phi^*\|_F^2 \leq \frac{288\sigma_1^2}{\sigma_r \kappa} \left(\frac{3}{4} + \frac{8T_0}{\kappa B} + \frac{2}{K\|\Sigma\|_2} \right) \frac{Kr \log(\frac{d_1+d_2}{\delta})}{B} S_2^4$$

with probability at least $1 - \delta$, where $S_2 = \max\{S_p, S_q\}$ is a constant.

Remark 2 (Initial Estimate Φ_0). Note that we require the initialization error $\|\Phi_0 - \Phi^*\|_F^2$ to be bounded. This assumption, often referred to as the ‘basin of attraction’ is a standard practice in the non-convex low-rank matrix estimation literature (Jain et al., 2013; Chi et al., 2019). It ensures that the iterative algorithm converges to the desired target. Such assumptions are valid in diverse situations, such as when offline data are available, or when the length of the exploration stage is large enough to provide a warm start for the gradient descent algorithm.

The initial estimator Φ_0 can also be chosen as the unconstrained maximum likelihood estimator (MLE) based on data collected during the exploration phase. Under standard regularity conditions for the MNL model, the unconstrained MLE achieves the convergence rate: $\|\hat{\Phi}_{MLE} - \Phi^*\|_F = O(\sqrt{d_1 d_2 / T_0})$ (Van der Vaart, 2000). Therefore, if the exploration length T_0 satisfies $T_0 \gtrsim d_1 d_2 / \sigma_r^2$, the unconstrained MLE will satisfy the initial condition.

Note that the result holds for an arbitrary choice of $B > 0$. Increasing B and therefore increasing the length of exploration T_0 will naturally decrease the estimation error. In this case, accurate estimation of the subspace will lead to better exploitation. However, increasing T_0 will also increase the total cumulative regret. Hence the choice of T_0 shows the exploration-exploitation trade-off. In our method, we choose the optimal length of exploration $T_0 = O(\sqrt{T})$ to minimize the cumulative regret. Finally, note that the rate is proportional to the rank r , which would have been scaling with $\min\{d_1, d_2\}$ without the low-rank assumption. This illustrates how the low-rank assumption plays a crucial role in reducing the estimation error.

Next we first establish confidence bound on the parameter θ_{rtv}^* .

Lemma 1 (Confidence bound on reduced space). Suppose Assumptions 1, 2 and 3 hold. Further

assume that $\|\Theta_{r+1:d_2, r+1:d_1}^*\|_F^2 \leq S_\perp$ for some S_\perp . Let $\widehat{\theta}_{n,rtv}$ be the maximum likelihood estimator of θ_{rtv}^* using observations from user $t = 1, \dots, n$ by minimizing (6). Then,

$$\|\widehat{\theta}_{n,rtv} - \theta_{rtv}^*\|_{W_n} \leq \frac{1}{\kappa n K} \left(\sigma \sqrt{2df \log \left(1 + \frac{n}{df} \right) + 4 \log n} + S_2^2 \cdot S_\perp \cdot \sqrt{nK} \right) =: \alpha_n$$

with probability at least $1 - 1/n^2$, where $W_n = \frac{1}{nK} \sum_{t=1}^n \sum_{i \in S_t} x_{it,rtv} x_{it,rtv}^\top$ and $df = (d_1 + d_2)r - r^2$ is the dimension of the reduced space.

With this definition of α_n , we can calculate the optimistic utility defined in (5). Finally, we establish a non-asymptotic upper bound on the cumulative regret of our ELSA-UCB algorithm.

Theorem 1 (Regret Bound of ELSA-UCB). *Suppose assumptions of Proposition 1 hold. Define*

$$\begin{aligned} T_0 &:= 4\sigma^2(C_1\sqrt{d_1d_2} + C_2\sqrt{\log T})^2 + \frac{2B}{\lambda_{\min}(\Sigma)K}, \\ S_\perp &:= \frac{288\sigma_1^3}{\sigma_r^3 \cdot \kappa} \cdot \left(\frac{3}{4} + \frac{8T_0}{\kappa B} + \frac{2}{K\|\Sigma\|_2} \right) \frac{Kr \log(\frac{d_1+d_2}{\delta})}{B} S_2^4, \\ \alpha_n &:= \frac{1}{\kappa} \left(\sigma \sqrt{2df \log \left(1 + \frac{n}{df} \right) + 4 \log n} + S_2^2 \cdot S_\perp \cdot \sqrt{nK} \right), \end{aligned}$$

for any $B > 0$, where $df = (d_1 + d_2)r - r^2$ is the degree of freedom on the reduced space. Then applying Algorithm 2 with T_0 and α_n , the cumulative regret of our ELSA-UCB policy satisfies

$$\mathcal{R}_T \leq R_{\max} \left(T_0 + 3 + 2\alpha_T \sqrt{T \cdot 2 \cdot df \log(T/df)} + 2S_2^2 S_\perp (T - T_0) \right),$$

where $R_{\max} = \max_{i \in [N]} r_i$.

Theorem 1 provides a detailed regret bound of our policy. When applying our policy to e-commerce applications with a large number of users (large T), we can further simplify this rate. With the choice $B = b\sqrt{T}$ for some constant b , we have $S_\perp = O(r/\sqrt{T})$ by definition and therefore the sub-linear regret $\mathcal{R}_T = \tilde{O}(r(d_1 + d_2)\sqrt{T})$, where $\tilde{O}(\cdot)$ ignores some logarithm term, which implies that the mean regret converges to 0 as $T \rightarrow \infty$. For d -dimensional contextual assortment problem, Chen et al. (2020) established an $\Omega(d\sqrt{T}/K)$ lower bound on the cumulative regret. As the capacity K is the maximum number of items that are displayed each time, we can interpret

K as a constant, and consequently, the lower bound becomes $\Omega(d\sqrt{T})$. When these results are applied by interpreting vectorization of the outer product of dual features as a single feature, the lower bound becomes $\Omega(d_1 d_2 \sqrt{T})$, without the low-rank assumption. Our algorithm significantly reduces the rate of regret to $\tilde{O}(df \cdot \sqrt{T})$ in the low-rank regime.

Establishing this regret bound possesses two main technical challenges. The first challenge involves incorporating the low-rank structure. To address this, we utilize results from the low-rank matrix estimation literature and adapt them to the LOAD problem. This enables us to establish an estimation bound on the estimated subspace. The second challenge arises from the inherent combinatorial structure of the assortment problem. To overcome this, we construct bound on the difference between the rewards in the original problem and the transformed problem in the reduced space, which enables us to establish regret bounds for our algorithm. We provide a proof sketch in Section S.7.1 of the Appendix.

5 Numerical Studies

In this section, we evaluate the cumulative regret of our ELSA-GIC policy across varying scenarios, including different numbers of users, feature dimensions, ranks of parameter matrix, numbers of items and capacity of the assortment. We begin by examining it using synthetic data in Section 5.1 and subsequently validate its practicability in a real-world dataset in Section 5.2.

5.1 Simulation

To generate the parameter matrix Φ^* , we first construct a diagonal matrix D^* with r non-zero components, each set to be 10. Next we multiply random orthonormal matrices $U^* \in \mathbb{R}^{d_2 \times r}$ and $V^* \in \mathbb{R}^{d_1 \times r}$ to generate a random rank- r matrix $\Phi^* = U^* D^* (V^*)^\top \in \mathbb{R}^{d_2 \times d_1}$. For the user features, we generate $q_t \in \mathbb{R}^{d_1}$ for every $t \in [T]$ from the d_1 -dimensional standard Gaussian distribution. Similarly, for item features, we generate $p_i \in \mathbb{R}^{d_2}$ from the d_2 -dimensional standard Gaussian distribution for every $i \in [N]$. Note that the N item features are fixed over the time horizon while

user features are generated at each time step. The revenue is set as $r_i = 1$ for every $i \in [N]$, following the setup in Oh and Iyengar (2021). This accounts for scenarios where the goal is to maximize the sum of binary outcomes, aiming to maximize the total number of conversions, such as clicks or purchases in online retail.

Utilizing the generated parameters and features, we simulate user choices and the corresponding assortment selections following the policy. We compare the performance of our proposed ELSA-UCB with the estimated rank from GIC (denoted ELSA-GIC) against two versions of the UCB-MNL (Agrawal et al., 2019; Oh and Iyengar, 2021). As UCB-MNL considers features for each user-item pair as x_{it} , we consider two formulations of the joint features; “stacked” and “vectorized”.

- **Stacked UCB-MNL:** As shown in Figure 2, we stack the user features and the item features together including intercept as $x_{it} = (1, p_i, q_t) = (1, p_{i1}, p_{i2}, \dots, p_{id_2}, q_{t1}, \dots, q_{td_1}) \in \mathbb{R}^{d_1+d_2+1}$, which allows the linear formulation of the utilities to take into account the main effects of both features with parameter $\theta = (\alpha, \beta_1, \dots, \beta_{d_2}, \gamma_1, \dots, \gamma_{d_1}) \in \mathbb{R}^{d_1+d_2+1}$:

$$v_{it} = \theta^\top x_{it} = \alpha + \sum_{j=1}^{d_2} p_{ij} \beta_j + \sum_{k=1}^{d_1} q_{tk} \gamma_k.$$

- **Vectorized UCB-MNL:** As shown in Figure 3, we consider the vectorization of the outer product of the dual features with intercept, $p'_i = (1, p_{i1}, \dots, p_{id_2})$ and $q'_t = (1, q_{t1}, \dots, q_{td_1})$:

$$X_{it} = p'_i \otimes q'_t = \begin{pmatrix} 1 & q_{t1} & \dots & q_{td_1} \\ p_{i1} & p_{i1}q_{t1} & \dots & p_{i1}q_{td_1} \\ \vdots & \vdots & \ddots & \vdots \\ p_{id_2} & p_{id_2}q_{t1} & \dots & p_{id_2}q_{td_1} \end{pmatrix} \in \mathbb{R}^{(d_2+1) \times (d_1+1)},$$

$$x_{it} = \text{vec}(X_{it}) = (1, p_{i1}, \dots, p_{id_2}q_{td_1}) \in \mathbb{R}^{(d_2+1)(d_1+1)},$$

as the joint feature for the user-item pair. This takes into account for the main effects and the interaction terms of the dual features with parameter $\theta = (\alpha, \dots, \delta_{11}, \dots, \delta_{d_2 d_1}) \in$

$\mathbb{R}^{(d_2+1)(d_1+1)}$, which leads to the following formulation of utilities:

$$v_{it} = \theta^\top x_{it} = \alpha + \sum_{j=1}^{d_2} p_{ij} \beta_j + \sum_{k=1}^{d_1} q_{tk} \gamma_k + \sum_{j=1}^{d_2} \sum_{k=1}^{d_1} \delta_{jk} p_{ij} q_{tk}.$$

Note that the stacked formulation can be viewed as a special case of the vectorized formulation, when there is no interaction. In this case, the parameter matrix contains non-zero elements only on the first row and the first column, which restricts the rank of the matrix to be at most 2.

We apply our proposed ELSA-GIC policy and the two variations of UCB-MNL as baselines for comparison. We repeat the simulation 50 times and plot the mean and 95% confidence interval of the cumulative regret for each $T \in \{1000, 2000, 3000, 5000, 7500, 10000\}$ under different environments.

First we demonstrate the consistency of rank-estimation through GIC (4). We fix $d_1 = 30, d_2 = 20, N = 20, K = 3, r = 3$ and change the number of users over $T = 100, 200, 500, 1000, 2000$ to compare the estimated rank when T increases. As shown in Figure 5, the probability of accurate rank estimation nearly converges to 1 as the sample size increases.

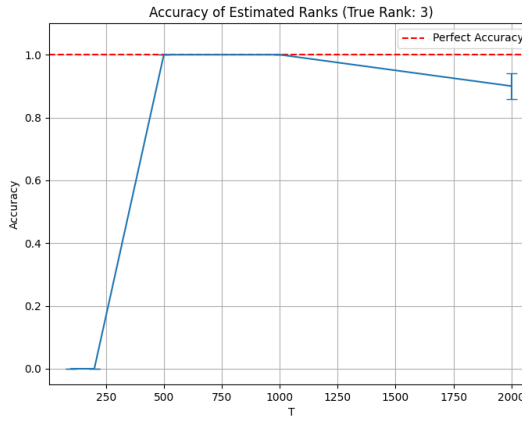


Figure 5: Accuracy of estimated rank using GIC with increasing T .

For the first line of experiments, to assess the performance in terms of cumulative regret, we fix $d_1 = 50, d_2 = 20, N = 20, K = 3$ and change the rank $r \in \{2, 5, 10\}$ and number of users over $T = 1000, 2000, 3000, 5000, 7500, 10000$ and plot the corresponding cumulative regret in Figure

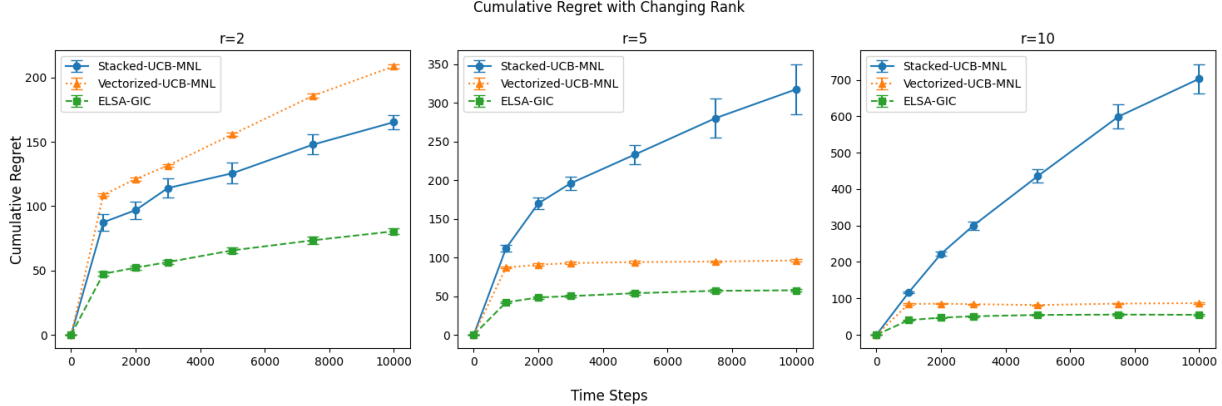


Figure 6: Cumulative regrets of our proposed ELSA-GIC algorithm compared with Stacked UCB-MNL and Vectorized UCB-MNL for different ranks $r \in \{2, 5, 10\}$.

6. In higher ranks, the Stacked UCB-MNL produces larger cumulative regret, as it does not take consideration for the diverse interactions between the dual features. On the other hand, the Vectorized UCB-MNL has comparable performance when the rank is high. However, when the rank is low, the performance of Vectorized UCB-MNL is not satisfactory. Our ELSA-GIC policy universally outperforms both methods as it utilizes the low-rank structure and therefore efficiently estimate how the interactions between the dual features affect user preference of items. We also note that the Stacked method corresponds to a special case with $r = 2$, which is only correctly specified when the true parameter matrix has nonzero entries solely in the main-effect terms, the first row and the first column. In our simulations, however, the parameter matrix includes nonzero interaction terms, so the Stacked method is mis-specified even when the true rank equals 2. Our method, in contrast, remains correctly specified in this case and achieves superior performance.

Note that the cumulative regrets across different settings are not directly comparable. For example, in Figure 6, we observe a decrease in cumulative regrets for our method as the rank increases. This phenomenon occurs as we fix the scale for the singular values of Φ^* , the intrinsic value v_{it} increases, making it be easier to distinguish the optimal assortments. However, if we decrease the scale of the singular values as rank increases, the scale of the intrinsic value might remain the same, but the parameter estimation becomes challenging, potentially leading to performance degradation.

Therefore, it would be fair to compare cumulative regret only within the same settings and compare the relative gap between different settings.

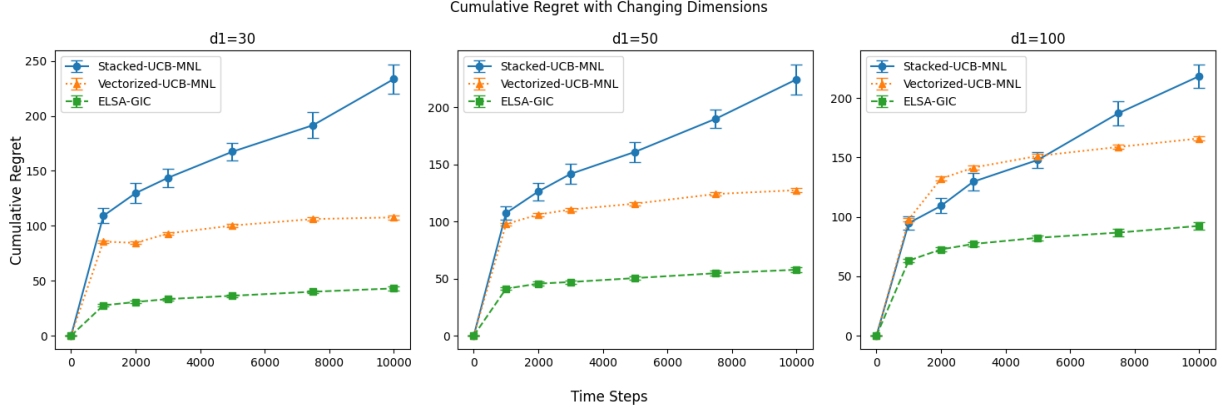


Figure 7: Plots of cumulative regret by T for different dimensions.

In the next set of experiments, we fix $d_2 = 20, r = 3, N = 20, K = 3$ while changing $d_1 \in \{30, 50, 100\}$. The results are shown in Figure 7. The Stacked UCB-MNL shows poor performance across all dimensions. Moreover, we can observe that the gap between the cumulative regret of ELSA-GIC and Vectorized UCB-MNL widens as d_1 increases. This indicates that our algorithm is even preferable in environments with higher dimensional features. Furthermore, note that the scale of the regret increases as d_1 increases which aligns with the results of Theorem 1.

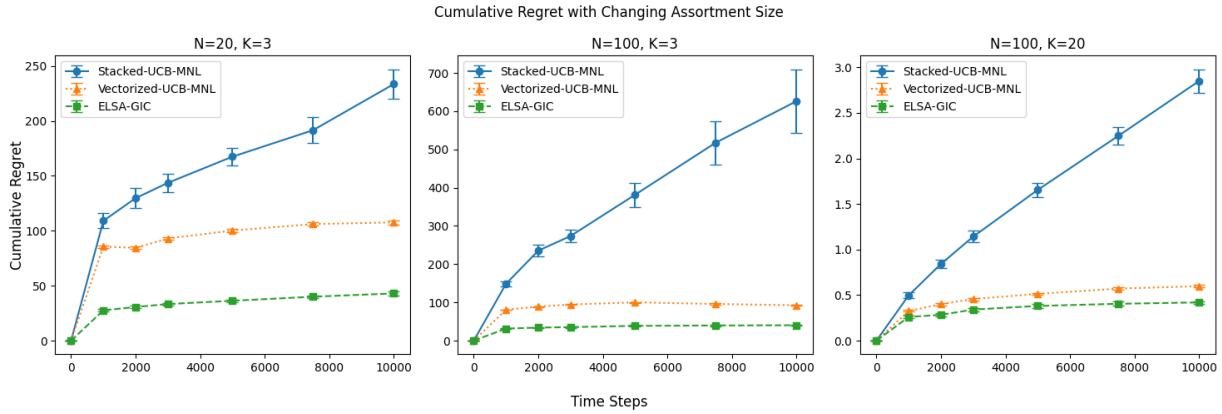


Figure 8: Plots of cumulative regret by T for different numbers of items and capacity.

In the third set of experiments, we fix $d_1 = 30, d_2 = 20, r = 3$ and change (N, K) to be

$\{(20, 3), (100, 3), (100, 20)\}$. The results are illustrated in Figure 8. Note that as the assortment capacity K increases, the gap between the optimal assortment and the near-optimal assortments decreases, resulting in smaller regrets. Overall, our proposed method outperforms both Stacked UCB-MNL and Vectorized UCB-MNL across all setups.

In the final set of experiments, we evaluate the robustness of ELSA-GIC under model misspecification. We consider three scenarios:

1. **Approximately low-rank Φ^* :** The first r singular values of Φ^* are fixed at a constant level, while the remaining singular values are set to be small - specifically, 1% of the leading singular values - capturing approximate low-rank structure with residual noise.
2. **Full-rank Φ^* :** The parameter matrix is drawn as a full-rank matrix without dominant singular directions, favoring the Vectorized UCB-MNL model, which does not assume any low-rank structure.
3. **Main-effect-only model:** The utility is generated without any interaction between user and item features and is influenced solely by the main effects. In this setting, the effective rank is 2, and the structure favors the Stacked UCB-MNL model.

We fix $(d_1, d_2, N, K) = (30, 20, 20, 3)$, and use $r = 3$ for the approximately low-rank matrix. As shown in Figure 9, ELSA-GIC achieves the lowest regret in the approximately low-rank case, demonstrating its strength when the low-rank assumption only holds approximately. Moreover, it remains competitive even when the data-generating process favors alternative models, achieving comparable regret to the specialized methods under their respective advantageous regimes.

5.2 Real Data Application

In this section, we apply our algorithm to the “Expedia Hotel” dataset (Adam et al., 2013) to evaluate its performance in real data.

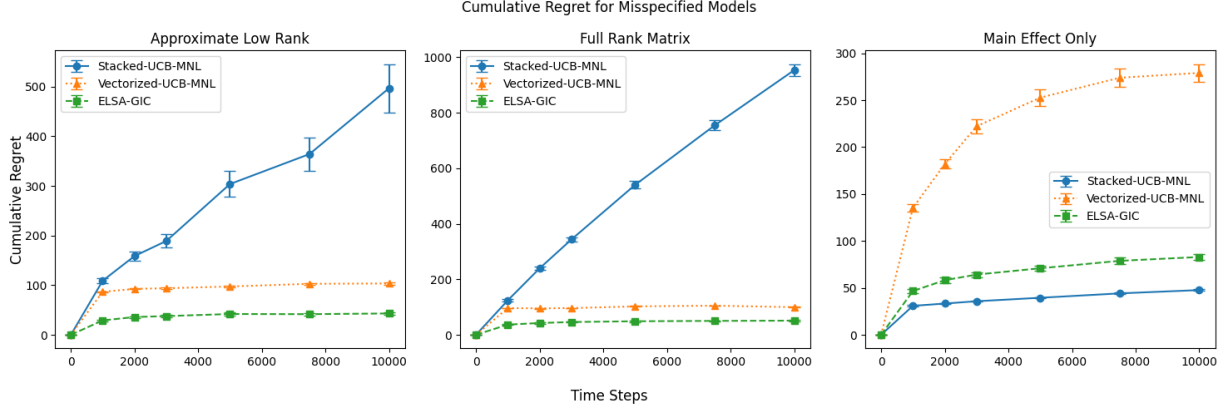


Figure 9: Cumulative regret over time T under various model misspecification settings.

5.2.1 Data Pre-processing

The dataset consists of 399,344 unique searches on 23,715 search destinations each accompanied by a recommendation of maximum 38 hotels from a pool of 136,886 unique properties. User responses are indicated by clicks or hotel room purchases. The dataset also includes features for each property-user pair, including hotel characteristics such as star ratings and location attractiveness, as well as user attributes such as average hotel star rating and prices from past booking history.

It is important to note that search queries constrain assortments to those within the search destination. We focus on data from the top destination with the highest search volume. Additionally, we filter out columns with missing over 90% of searches. To address missing values in the remaining data for average star ratings and prices of each user from historical data, we employ a simple regression tree imputation. For hotel features, we compute the mean of feature values across searches. We discretize numerical features such as star ratings or review scores into categories to improve model fitting. After pre-processing, we have $T = 4465$ unique searches encompassing $N = 124$ different hotels, with $d_2 = 10$ hotel features and $d_1 = 18$ user features. The description of features is given in Table 1. We normalize each feature to have mean 0 and variance 1. As for the item features, we truncate the feature values to lie within $[-3, 3]$ to avoid the effect of outliers.

Item (Hotel) Features	Star rating (4 levels), Average review score (3 levels), Brand of property, Location score, Log historical price, Current price, Promotion
User (Search) Features	Length of stay (4 levels), Time until actual stay (4 levels), # of adults (3 levels), # of children (3 levels), # of rooms (2 levels), Inclusion of Saturday night, Website domain, User historical star rating (3 levels), User historical price (4 levels)

Table 1: Table of item and user features.

5.2.2 Analysis of the Expedia Dataset

To evaluate different dynamic assortment selection policies, we first estimate the ground truth parameter Φ^* using rank-constrained maximum likelihood estimation (1) on the full dataset. Consequently, the Generalized Information Criterion (GIC) selects a rank of $r = 5$ across a range of candidate ranks. Following the procedure used in our simulation studies, we compare the cumulative regrets of our proposed ELSA-GIC policy with rank estimation against Stacked UCB-MNL and Vectorized UCB-MNL. We evaluate the algorithms at different time horizons $T \in \{2000, 5000, 10000\}$. To assess the performance of the algorithm over an extended time horizon, we resample the users based on the original dataset.

Number of Samples	vs. Stacked-UCB-MNL	vs. Vect-UCB-MNL
2000	26.3 % ($\pm 1.0 \%$)	2.5 % ($\pm 0.7 \%$)
5000	45.8 % ($\pm 1.0 \%$)	3.1 % ($\pm 1.0 \%$)
10000	61.8 % ($\pm 0.8 \%$)	3.5 % ($\pm 1.4 \%$)

Table 2: Performance improvement of our algorithm over baseline methods.

As shown in Table 2, our proposed ELSA-GIC algorithm outperforms both Stacked UCB-MNL and Vectorized UCB-MNL in terms of cumulative regret. Notably, the performance gap between ELSA-GIC and the baseline methods widen as the time horizon increases. Even though the real dataset does not exhibit a strictly low-rank structure relative to its dimensions ($r = 5$ vs. $(d_1, d_2) = (18, 10)$), our method still achieves superior performance. By avoiding unnecessary full-dimensional estimation and instead concentrating learning within a reduced subspace, ELSA-GIC effectively improves the cumulative reward compared to the baseline methods.

Acknowledgments

The authors would like to thank the editor, associate editor, and reviewers for their insightful comments, which have greatly improved the presentation. The research was partially supported by NSF grant SES 2217440.

Supplementary Materials

“Low-Rank Online Dynamic Assortment with Dual Contextual Information”

In this supplement, we first discuss and compare additional related works in Section S.1. We provide high probability regret bound in S.2. Next, we provide sensitivity analysis regarding the hyperparameters of UCB in Section S.3. We also discuss the implementation of UCB-MNL, the baseline algorithm for comparison in S.4, and provide the detailed rank tuning implementation and the batch extension of our algorithm in Section S.5. A few interesting future directions are provided in Section S.6. Finally, we include detailed proofs of the theorems and lemmas in Section S.7.

S.1 Additional Related Work

In this section, we introduce and discuss the distinction with related works in the literature on low-rank bandits, bandits with sparsity assumption and recommendation systems.

S.1.1 Comparison with Low-rank Bandits

Here, we highlight the distinction between our work and existing literature in bandit problems.

1. **Theoretical distinction from bilinear bandits:** We now clearly articulate the key differences between our setting and the bilinear bandit literature (e.g., Jun et al. (2019)) in both theory and methodology. In particular, we highlight how the MNL feedback model, the combinatorial action space of assortments, and the non-linear reward structure lead to substantial differences in problem formulation, analysis, and algorithm design. These distinctions are now discussed in detail in our response to your next comment.
2. **Algorithmic structure and adaptation:** While the factored gradient descent (FGD) algorithm we adopt for subspace estimation is indeed rooted in the low-rank matrix literature,

our analysis tailors it to the categorical MNL feedback setting and proves convergence properties specific to this structure. Furthermore, our ELSA-UCB framework departs from existing two-stage bandits by incorporating a confidence-adjusted refinement over a learned low-rank subspace with categorical choice-based feedback. This leads to a new regret decomposition and necessitates novel bounding techniques.

S.1.2 Comparison with Sparsity Assumption

Both low-rank and sparse structures are widely used to address high dimensionality in statistical learning. Prior works such as Udell and Townsend (2019), Koren et al. (2009), and Bell and Koren (2007) support the presence of low-rank structures in high-dimensional settings, particularly in recommendation systems. On the other hand, sparsity assumptions have also been effectively employed in contextual dynamic assortment optimization, as seen in Wang et al. (2019) and Shao et al. (2022), where LASSO-based methods are used to reduce sample complexity. In this work, we focus on the low-rank structure for two main reasons:

- **Matrix structure and bilinear modeling:** A sparsity assumption on the parameter matrix Φ^* is equivalent to a sparsity assumption on the vectorized parameter matrix $\text{vec}(\Phi^*)$. This facilitates the use of standard sparse bandit techniques. In contrast, the low-rank assumption explicitly leverages the matrix structure of Φ^* . This structural difference motivates the development of new theory and algorithms tailored to low-rank structure, as undertaken in our work.
- **Interpretability through latent subspaces:** The low-rank assumption enables learning of intrinsic latent representations of both user and item features. In particular, it reveals low-dimensional subspaces that drive user–item interactions, offering a more interpretable and compact model of preference formation. In contrast, sparsity implies that only a small number of feature pairs affect preference, without identifying coherent subspace structure. This

difference is particularly important in dual-context environments, where subspace learning can enhance both prediction and generalization.

S.1.3 Recommendation Systems

Recommendation system is a field with extensive research closely related to the dynamic assortment selection problem. These systems collect user preferences across a range of items and forecast these preferences. Multiple methodologies were developed for recommendation systems, including content-based filtering, demographic filtering, and collaborative filtering methods (Bobadilla et al., 2013; Dai et al., 2019, 2021). Content-based filtering tailors personalized recommendations by drawing insight from user’s history, suggesting similar items based on their previous choices (Van Meteren and Van Someren, 2000). In contrast, collaborative filtering observes user ratings on items and then offers recommendations for each user by drawing data from similar users. To mitigate issues arising from the sparsity of observations, dimension reduction techniques including low-rank matrix factorization (Sarwar et al., 2000) and covariate-assisted matrix completion (Robin et al., 2018; Mao et al., 2019; Ibriga and Sun, 2023) have been applied to learn user preferences. However, in the dynamic assortment problem, the decision maker can only observe binary outcomes of user choices, which are limited to at most one selection per user, without any quantitative observations such as user ratings. This line of literature motivates us to investigate the dynamic assortment problem, involving user-item interactions to model user preferences toward items.

S.2 High Probability Bound of Regret

Here we provide results involving high probability bounds rather than bounds on the expectation of the regret in Corollary 1.

Corollary 1 (High Probability Bound of Regret). *Suppose assumptions of Proposition 1 hold.*

Define

$$\begin{aligned}
T_0 &:= 4\sigma^2(C_1\sqrt{d_1d_2} + C_2\sqrt{\log T})^2 + \frac{2B}{\lambda_{\min}(\Sigma)K}, \\
S_{\perp} &:= \frac{288\sigma_1^3}{\sigma_r^3 \cdot \kappa} \cdot \left(\frac{3}{4} + \frac{8T_0}{\kappa B} + \frac{2}{K\|\Sigma\|_2} \right) \frac{Kr \log(\frac{d_1+d_2}{\delta})}{B} S_2^4, \\
\alpha_n &:= \frac{1}{\kappa} \left(\sigma \sqrt{2df \log \left(1 + \frac{n}{df} \right)} + 4 \log n + S_2^2 \cdot S_{\perp} \cdot \sqrt{nK} \right),
\end{aligned}$$

for any $B > 0$, where $df = (d_1 + d_2)r - r^2$ is the degree of freedom on the reduced space. Then by applying Algorithm 2 with $T_0 > 1/\delta$ and α_n , the cumulative regret of our ELSA-UCB policy satisfies

$$\sum_{t=1}^T r_t \leq R_{\max} \left(T_0 + 2\alpha_T \sqrt{T \cdot 2 \cdot df \log(T/df)} + 2S_2^2 S_{\perp} (T - T_0) \right),$$

with probability at least $1 - 2\delta$, where $R_{\max} = \max_{i \in [N]} r_i$.

The proof is provided in Appendix S.7.

S.3 Sensitivity Analysis of Hyperparameters

S.3.1 Confidence Bound Related Hyperparameters

In this section, we provide a detailed description of the tuning parameter choices for the ELSA-UCB algorithm as well as implementation details for the Stacked UCB-MNL and Vectorized UCB-MNL baselines. The confidence radius in ELSA-UCB is based on Lemma 1 and is defined as follows:

$$\|\widehat{\theta}_{n,rtv} - \theta_{rtv}^*\|_{W_n} \leq \frac{1}{\kappa n K} \left(\sigma \sqrt{2df \log \left(1 + \frac{n}{df} \right)} + 4 \log n + S_2^2 \cdot S_{\perp} \cdot \sqrt{nK} \right) =: \alpha_n.$$

To simplify tuning, we reparametrize α_n as:

$$\alpha_n = \alpha \sqrt{2df \log(1 + n/df) + 4 \log n} + \beta \sqrt{nK},$$

where α, β are tuning parameters. The first term mirrors the confidence radius used in UCB-MNL from Oh and Iyengar (2021), and we use the same value across different methods. The second term accounts for the approximation error due to truncation. We perform a grid search over different values of (α, β) with $d_1 = 50, d_2 = 20, r = 3$ to assess sensitivity and find the algorithm to be robust across a range of parameters. First we fix $\beta = 1$ and compare the regrets over $\alpha \in \{2, 5, 10\}$, as shown in the left plot of Figure 10. Next, we compare the regrets over $\beta \in \{0.5, 1.0, 2.0\}$, as shown in the right plot of Figure 10. We can verify that the performance of our algorithm is robust over the selection of hyperparameters. The final values $(\alpha, \beta) = (5, 1)$ are used in all reported simulations.

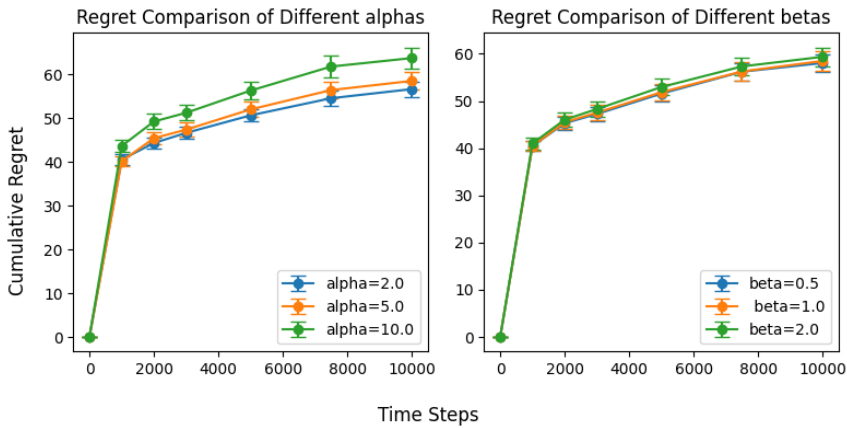


Figure 10: Cumulative regrets for different α, β .

S.3.2 Exploration Length Related Hyperparameters

As discussed in Theorem 1, the choice of the initial exploration length $T_0 = cd_1d_2 + \sqrt{T}$ balances the trade-off between obtaining a reliable estimate of the low-rank structure and minimizing regret accumulated during random exploration. In our simulations, we fix $c = 0.2$. To examine sensitivity to this parameter, we conducted simulations varying the constant $c \in \{0.1, 0.2, 0.5\}$.

The results, shown in Figure 11, demonstrate that our method achieves consistently low regret across a range of values of c . This confirms that the theoretical guideline provides a robust and practical choice for T_0 .

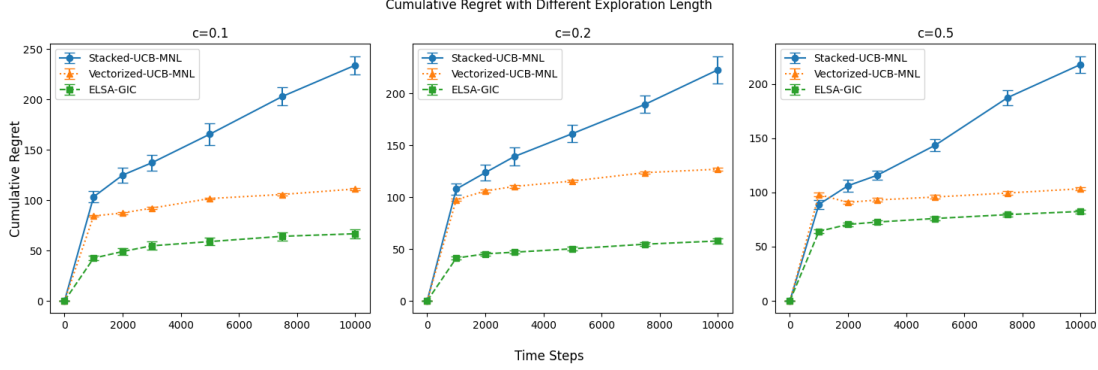


Figure 11: Cumulative regret by T for different choices of the exploration parameter c .

S.4 Implementation of UCB-MNL

In this section, we introduce UCB-MNL from Oh and Iyengar (2021) and how it is implemented for Stacked UCB-MNL and Vectorized UCB-MNL, as shown in Algorithm 3.

Algorithm 3 UCB-MNL (Oh and Iyengar, 2021)

Input: Initialization T_0 , confidence radius α_t .

- 1: For $t \in [T_0]$
- 2: Randomly choose S_t with $|S_t| = K$
- 3: $V_t \leftarrow V_{t-1} + \sum_{i \in S_t} x_{it} x_{it}^\top$
- 4: **for** $\text{dot} = T_0 + 1, \dots, T$,
- 5: Compute $z_{it} = x_{it}^\top \hat{\theta}_{t-1} + \alpha_t \|x_{it}\|_{V_{t-1}^{-1}}$ for all i
- 6: Offer $S_t = \arg \max_S \tilde{R}_t(S)$ and observe y_t
- 7: Update $V_t \leftarrow V_{t-1} + \sum_{i \in S_t} x_{it} x_{it}^\top$
- 8: Compute MLE $\hat{\theta}_t$
- 9: **end for**

The notations $\tilde{R}_t(S)$ and α_t in Algorithm 3 are define as:

$$\tilde{R}_t(S) := \frac{\sum_{i \in S} r_{it} \exp(z_{it})}{1 + \sum_{j \in S} \exp(z_{jt})},$$

and $\alpha_t = \frac{1}{2\kappa} \sqrt{2d \log(1 + \frac{t}{d}) + 2 \log t}$.

The only difference between the Stacked and Vectorized versions lies in the construction of the context vector x_{it} :

- For Vectorized UCB-MNL, we use $x_{it} = \text{vec}(p_i q_t^\top)$.
- For Stacked UCB-MNL, we use $x_{it} = (p_i^\top, q_t^\top)^\top$, i.e., the concatenation of the two context vectors.

S.5 Additional Algorithms

In this section, we provide details of the sub-algorithm STATICMNL from Rusmevichientong et al. (2010), our ELSA-UCB algorithm with rank estimation, and the batch version of ELSA-UCB.

S.5.1 STATICMNL

Here we discuss and provide details of STATICMNL in Algorithm 4. The STATICMNL algorithm is used to compute the optimal assortment under the Multinomial Logit (MNL) model, given a fixed utility vector $\mathbf{v} = (v_1, \dots, v_N)$ and reward vector $\mathbf{r} = (r_1, \dots, r_N)$, subject to a capacity constraint K . Instead of exhaustively enumerating all $\sum_{k=1}^K \binom{N}{k}$ possible subsets (which is computationally heavy), the algorithm identifies a much smaller set of candidate assortments—specifically, $O(N^2)$ candidates, by iteratively examining intersection points that determine changes in the ranking of marginal value contributions.

The algorithm involves sorting utilities and intersection points, and updating candidate assortments accordingly. The resulting computational complexity is $O(N^2)$, ignoring logarithmic factors, which makes STATICMNL a computationally efficient subroutine for solving the inner maximization in our UCB-based stage. It is also worth noting that the algorithm does not have a dependency on K .

S.5.2 ELSA-UCB with Rank Estimation

The first extension is the ELSA-UCB algorithm with rank estimation using GIC. We use the samples from random exploration to estimate the rank. We provide theoretical results on rank estimation using GIC in Proposition 2.

Algorithm 4 STATICMNL

Input: Assortment capacity K , utility vector $v = (v_1, \dots, v_N)$, reward vector $r = (r_1, \dots, r_N)$.

- 1: For each $j \in [N]$, define $I(0, j) = r_j$ and for $i, j \in [N]$ with $i \neq j$, define $I(i, j) = (v_i w_i - v_j w_j) / (v_i - v_j)$.
- 2: Denote $L = N(N+1)/2$. Sort the pairs to $(i_1, j_1), \dots, (i_L, j_L)$ so that $0 \leq i_l < j_l \leq N$ for every $l \in [L]$ and

$$-\infty \equiv I(i_0, j_0) < I(i_1, j_1) \leq \dots \leq I(i_L, j_L) < I(i_{L+1}, j_{L+1}) \equiv +\infty$$

- 3: Sort the items based on v_i so that $v_{\sigma_1^0} \geq v_{\sigma_2^0} \geq \dots \geq v_{\sigma_N^0}$.
- 4: Let $A^0 = G^0 = \{\sigma_1^0, \dots, \sigma_K^0\}$ and $B^0 = \emptyset$.
- 5: **for** $t = 1, \dots, L$, **do**
- 6: If $i_t \neq 0$, let σ_t be the permutation obtained from transposing i_t and j_t from σ^{t-1} , and set $B^t = B^{t-1}$.
- 7: If $i_t = 0$, let $\sigma^t = \sigma^{t-1}$ and $B^t = B^{t-1} \cup \{j_t\}$.
- 8: Let $G_t = \{\sigma_1^t, \dots, \sigma_K^t\}$ and $A^t = G^t \setminus B^t$.
- 9: **end for**
- 10: Find A_l with the maximum expected reward, i.e., $l^* = \arg \max_{l=0, \dots, L} R(A_l)$.
- 11: **return** A_{l^*}

Proposition 2 (Consistency of Rank Estimation). Define $GIC(r) := \mathcal{L}_n(\hat{\Phi}_r) - a_n \cdot (d_1 + d_2 - r) \cdot r$, where $a_n = O(1)$ and $na_n \rightarrow \infty$ as $n \rightarrow \infty$. Let $\hat{r} = \arg \min GIC(r)$. Then as $n \rightarrow \infty$, $\hat{r} \rightarrow r^*$.

To prove the consistency of the estimated rank, we first identify that the unconstrained MLE is consistent. Then by utilizing the strong convexity and smoothness of the negative log-likelihood function, we prove that the estimation error for the rank-constrained MLE with an over-specified rank is also consistent. Next we show that the estimation error for under-specified rank is lower bounded by a constant that depends on the last singular values of the matrix. Then, we finally prove that the GIC is minimized only at the true rank when the number of samples is sufficiently large. The detailed proof is provided in Appendix S.7.6.

S.5.3 ELSA-UCB with Batches

There are scenarios where users arrive in batches, i.e., multiple users arrive at each time point. Under this scenario, the agent cannot update the parameters for every user, but can only update

Algorithm 5 ELSA-GIC : ELSA-UCB with GIC Rank Estimation

Input: Assortment capacity K , learning rate η , initial parameter estimate Φ_0 and exploration length T_0 .

- 1: Observe item feature vectors $p_i, i \in [N]$.
- 2: **for** $t = 1, \dots, T_0$, **do**
- 3: Observe the current user feature vector q_t .
- 4: Randomly select a size K assortment $S_t \in \mathcal{S}$ and observe user choice \mathbf{y}_t .
- 5: **end for**
- 6: Estimate the rank \hat{r} using GIC (4) using the T_0 samples.
- 7: Estimate the low-rank matrix $\hat{\Phi} = \arg \max_{rk(\Phi)=\hat{r}} \mathcal{L}_n(\Phi)$ using Algorithm 1.
- 8: Estimate the subspace using SVD $\hat{\Phi} = \hat{U} \hat{D} \hat{V}^\top$.
- 9: Initialize $\hat{\theta}_{t,rtv} \in \mathbb{R}^k$ as the truncated vectorization of \hat{D} as in (3).
- 10: Rotate the item features $p'_i = \hat{U}^\top p_i$ for $i \in [N]$.
- 11: **for** $t = T_0 + 1, \dots, T$, **do**
- 12: Observe user feature vector q_t
- 13: Rotate the user feature $q'_t = \hat{V}^\top q_t$.
- 14: Compute $x_{it,rtv}$, the truncated vectorization of $p'_i(q'_t)^\top$ as in (3).
- 15: Compute $z_{it} = x_{it,rtv}^\top \hat{\theta}_{t,rtv} + \beta_{it}$ as in (5).
- 16: Select $S_t = \arg \max_S \tilde{R}_t(S)$ via StaticMNL and observe choice \mathbf{y}_t .
- 17: Update the MLE $\hat{\theta}_{t,rtv}$ by solving (6).
- 18: **end for**

after each batch. We provide the details of the algorithm under this scenario. Note that similar theoretical results hold when batch size is a constant, as the estimation bound holds at each end of the batch.

S.6 Future Directions

First, from a theoretical standpoint, it would be valuable to investigate the precise dependence of the regret bound on the assortment capacity parameter K . The current regret bound is not tight on the assortment capacity K , and sharper bounds that explicitly characterize this dependence may yield deeper insights. Additionally, it is worth exploring more sophisticated initialization strategies for low-rank models. In particular, recent work by Wang et al. (2017) suggests that projecting an unconstrained estimator onto a low-rank subspace can significantly reduce sample complexity, a technique that may be applicable to our framework with appropriate adaptation.

Algorithm 6 ELSA-UCB with Batches

Input: Assortment capacity K , rank of parameter matrix r , learning rate η , initial parameter estimate Φ_0 and exploration length B_0 .

- 1: Observe item feature vectors $p_i, i \in [N]$.
- 2: **for** $b = 1, \dots, B_0$, **do**
- 3: Observe the user feature vectors $q_t, t = N_{b-1} + 1, \dots, N_b$.
- 4: Randomly select a size K assortment $S_t \in \mathcal{S}$ for each user $t = N_{b-1} + 1, \dots, N_b$.
- 5: Observe user choices \mathbf{y}_t for each user $t = N_{b-1} + 1, \dots, N_b$.
- 6: **end for**
- 7: Estimate the low-rank matrix $\hat{\Phi} = \arg \max_{rk(\Phi)=r} \mathcal{L}_n(\Phi)$ using Algorithm 1.
- 8: Estimate the subspace using SVD $\hat{\Phi} = \hat{U} \hat{D} \hat{V}^\top$.
- 9: Initialize $\hat{\theta}_{t,rtv} \in \mathbb{R}^k$ as the truncated vectorization of \hat{D} as in (3).
- 10: Rotate the item features $p'_i = \hat{U}^\top p_i$ for $i \in [N]$.
- 11: **for** $b = B_0 + 1, \dots, B$, **do**
- 12: Observe user feature vectors q_t for each user $t = N_{b-1} + 1, \dots, N_b$.
- 13: Rotate the user features $q'_t = \hat{V}^\top q_t$ for every user $t = N_{b-1} + 1, \dots, N_b$.
- 14: Compute $x_{it,rtv}$, the truncated vectorization of $p'_i(q'_t)^\top$ as in (3).
- 15: Compute $z_{it} = x_{it,rtv}^\top \hat{\theta}_{t,rtv} + \beta_{it}$ as in (5).
- 16: Select $S_t = \arg \max_S \tilde{R}_t(S)$ via StaticMNL for each user $t = N_{b-1} + 1, \dots, N_b$.
- 17: Observe the batch choice \mathbf{y}_t for each user $t = N_{b-1} + 1, \dots, N_b$.
- 18: Update the MLE $\hat{\theta}_{t,rtv}$ by solving (6).
- 19: **end for**

Second, although our model accommodates dynamic user and item contexts, our current theoretical analysis assumes a fixed item catalog. In many real-world applications, however, the set of available items evolves over time. Unlike the non-contextual case, where new items require re-learning from scratch, contextual models enable the estimation of utilities for new items using their feature vectors, thereby supporting more efficient adaptation in dynamic environments.

Finally, extending the framework to incorporate pricing decisions offers another compelling direction. Pricing plays a dual role: it influences user preferences (and thus utilities) and directly affects revenue. Several recent works have explored pricing under fixed or linear models (Javanmard et al., 2020; Goyal and Perivier, 2022; Cai et al., 2023; Luo et al., 2024), but relatively little is known about joint assortment-pricing strategies in high-dimensional or dual-contextual settings. Investigating regret-minimizing algorithms for joint dynamic pricing and assortment optimization

in such environments remains an open and important challenge.

S.7 Technical Proofs

In this section, we provide technical proofs of the main theoretical statements:

S.7.2 Estimation Bound for Low-Rank Optimization: Proof of Proposition 1.

S.7.3 Bound on Error Induced by Truncation: Proof of Proposition 3.

S.7.4 Regret Upper Bound for the ELSA-UCB Policy: Proof of Theorem 1.

S.7.5 High Probability Bound for Regret of ELSA-UCB Policy: Proof of Corollary 1.

S.7.6 Proof of Rank Consistency using GIC: Proof of Proposition 3.

S.7.1 Proof Sketch of Regret Bound

This section provides an outline of the three major steps in the proof of Theorem 1. Detailed proofs are presented in Section S.7 of the Appendix. Step 1, as shown in Proposition 1, establishes a bound on the bias induced from rotation and truncation of the parameter matrix. Step 2 shows a bound on the difference between the optimistic utility z_{it} defined as (5) and the true utility v_{it} (Lemma 2). Finally, using this bound on the optimistic utility, Step 3 derives a bound on the regret of the t -th user, and the final result on the bound of cumulative regret (Theorem 1).

As our proposed algorithm ELSA-UCB truncates the lower right sub-block matrix of the rotated matrix, it is sufficient to establish a bound on the sub-block matrix.

Proposition 3 (Bounds for Subspace Estimation). *Suppose assumptions of Proposition 1 hold.*

Further assume the exploration length T_0 satisfies

$$T_0 \geq 4\sigma^2(C_1\sqrt{d_1d_2} + C_2\sqrt{\log(1/\delta)})^2 + \frac{2B}{\lambda_{\min}(\Sigma)K},$$

for some constants C_1, C_2 and any $\delta \in (0, 1)$, $B > 0$. Denote the SVD of the rank-constrained estimator as $\hat{U}\hat{D}\hat{V}^\top$. Then rotated true parameter $\Theta^* = \hat{U}^\top\Phi^*\hat{V}$ satisfies

$$\|\Theta_{r+1:d_2,r+1:d_1}^*\|_F^2 \leq \frac{288\sigma_1^3}{\sigma_r^3 \cdot \kappa} \cdot \left(\frac{3}{4} + \frac{8T_0}{\kappa B} + \frac{2}{K\|\Sigma\|_2} \right) \frac{Kr \log(\frac{d_1+d_2}{\delta})}{B} S_2^4 =: S_\perp \quad (\text{S1})$$

with probability at least $1 - \delta$.

Proposition 3 allows us to control the gap S_\perp between the reduced subspace and the original subspace by controlling B , which relates to the exploration length. Next, we establish a bound on the difference between the optimistic utility $z_{it} = x_{it,rtv}^\top \hat{\theta}_{t,rtv} + \alpha_t \cdot \|x_{it,rtv}\|_{W_t^{-1}}$ and the true utility $v_{it} = \langle X_{it}, \Theta^* \rangle$ using Proposition 3.

Lemma 2 (Bound on Optimistic Utility). *Let $z_{it} = x_{it,rtv}^\top \hat{\theta}_{t,rtv} + \beta_{it}$. Then for every $i \in [N]$,*

$$0 \leq z_{it} - \langle X_{it}, \Theta^* \rangle \leq 2\beta_{it} = 2\alpha_t \|x_{it,rtv}\|_{W_t^{-1}} + 2S_2^2 \cdot S_\perp$$

with probability at least $1 - t^{-2}$.

Note that z_{it} is greater than the true utility $v_{it} = \langle X_{it}, \Theta^* \rangle$ of item i to user t with probability at least $1 - t^{-2}$. Let us denote $R(\{w_i\}, S)$ as the expected revenue of offering assortment S under the MNL model assuming utility w_i for each item. Let S_t^* be the optimal assortment with respect to the true revenue v_{it} and S_t be the optimal assortment with respect to the optimistic revenue z_{it} . Then from the definition we have the following bound for regret r_t for user t :

$$r_t = R(\{v_{it}\}, S_t^*) - R(\{v_{it}\}, S_t) \leq R(\{z_{it}\}, S_t^*) - R(\{v_{it}\}, S_t) \leq R(\{z_{it}\}, S_t) - R(\{v_{it}\}, S_t). \quad (\text{S2})$$

Moreover, we can bound the last term using the result from Oh and Iyengar (2021) that establishes a bound on the difference of expected reward of an assortment given different utilities:

Lemma 3 (Lemma 5 of Oh and Iyengar (2021)). *Let $u_i, u'_i, i \in [N]$ be utilities and suppose $0 \leq r_i \leq R$ for every item $i \in [N]$. Then $R(\{u_i\}, S) - R(\{u'_i\}, S) \leq R \cdot \max_{i \in S} |u_i - u'_i|$.*

Combining (S2), Lemmas 2 and 3, we have

$$\begin{aligned}\mathcal{R}_T &= \sum_{t=1}^{T_0} r_t + \sum_{t=T_0+1}^T r_t \\ &\leq R_{\max} T_0 + R_{\max} \left(\sum_{t=T_0+1}^T 2\alpha_t \max_{i \in S_t} \|x_{it,rtv}\|_{W_t^{-1}} + 2S_2^2 S_{\perp} (T - T_0) \right).\end{aligned}$$

Lastly, presenting an upper bound on $\sum_{t=T_0+1}^T 2\alpha_t \max_{i \in S_t} \|x_{it,rtv}\|_{W_t^{-1}}$, we obtain our final result Theorem 1. Detailed proofs of the theoretical results are presented in Section S.7.

S.7.2 Proof of Proposition 1

S.7.2.1 Sketch of Proof for Proposition 1

Proof of Proposition 1 consists of three main steps. The first step is establishing a one-step bound of Algorithm 1 (Lemma 4 - 6). Next, we establish bounds on the eigenvalues of V_n (Lemma 8) to verify the constants of Lemma 5. Finally we extend the one-step result to the converged parameter (Lemma 7) to achieve Proposition 1.

We begin by re-stating the results on convergence of factored gradient descent algorithm on general loss functions from Zhang et al. (2023). Since the result on Zhang et al. (2023) is a general result for where the loss is a joint function of a low-rank matrix and a sparse tensor, we state the simplified result without the assumptions on the tensor portion. First we define the minimal Frobenius norm under rotation.

Definition 1. For $Z_1, Z_2 \in \mathbb{R}^{d \times r}$, $d(Z_1, Z_2)$ is defined as the minimal Frobenius norm between Z_1 and Z_2 under rotation i.e.,

$$d(Z_1, Z_2) = \min_{R \in \mathbb{Q}_r} \|Z_1 - Z_2 R\|_F,$$

where \mathbb{Q}_r is the space of r -dimensional rotation matrices, i.e., $\mathbb{Q}_r = \{R \in \mathbb{R}^{r \times r} : R^\top R = R R^\top = I_r\}$.

Next we use the following Lemma to illustrate the one-step rate decrease in terms of the new metric.

Lemma 4 (Lemma 1 from (Zhang et al., 2023)). *Suppose ℓ satisfies the restricted convexity and restricted smoothness i.e., for any matrices $\Phi_1, \Phi_2 \in \mathbb{B}(\Phi^*, \kappa_1)$ with rank at most r ,*

$$\frac{\mu}{2} \|\Phi_2 - \Phi_1\|_F^2 \leq \ell(\Phi_2) - \ell(\Phi_1) - \langle \nabla \ell(\Phi_1), \Phi_2 - \Phi_1 \rangle \leq \frac{L}{2} \|\Phi_2 - \Phi_1\|_F^2.$$

Let $\sigma_1, \dots, \sigma_r$ denote the singular values of Φ^* . Let c_1, c_2 be a constant such that $c_1 \leq \min\{1/32, \mu/(192L^2)\}$, $c_2 \leq \sqrt{\min\{\mu, 2\}(6L + 4)}$ and consider the step size $\delta = c_1/\sigma_1$. Let $Z^* = [U^*; V^*]$, and $Z^{(t)} = [U^{(t)}, V^{(t)}]$. If $d(Z^{(t)}, Z^*) \leq c_2\sqrt{\sigma_r}$, then Algorithm 1 satisfies

$$d^2(Z^{(t+1)}, Z^*) \leq \rho d^2(Z^{(t)}, Z^*) - \frac{\delta\mu}{4} \|\Phi^{(t)} - \Phi^*\|_F^2 + C_1 \|\nabla \ell(\Phi^*)\|_2^2,$$

where $\rho = 1 - \delta\mu\sigma_r/16$, $C_1 = 48r\delta^2\sigma_1 + 2\delta(8r/\mu + r/L)$.

Next step is checking the assumptions of Lemma 4. First we begin with defining V_n , which explains the variability of the features:

$$V_n := \sum_{t=1}^n \sum_{i \in S_t} x_{it} x_{it}^\top.$$

Then we have the following result on the restricted strong convexity and smoothness of the loss function:

Lemma 5 (Restricted Strong Convexity and Smoothness).

$$\frac{\kappa}{n} \lambda_{\min}(V_n) \|Y - X\|_F^2 \leq \mathcal{L}_n(Y) - \mathcal{L}_n(X) - \langle \nabla \mathcal{L}_n(X), Y - X \rangle \leq \frac{1}{n} \lambda_{\max}(V_n) \|Y - X\|_F^2,$$

as long as we can guarantee $x, y \in \mathcal{B}(\phi^*, 1)$, or equivalently $X, Y \in \mathcal{B}_F(\Phi^*, 1)$.

Next to utilize the result of Lemma 4, we need a bound on the last term of the inequality, the gradient of the loss function evaluated in the true parameter.

Lemma 6 (Bounded Gradient).

$$\left\| \frac{1}{n} \sum_{t=1}^n \sum_{i \in S_t} (y_{it} - p_t(i|\Phi^*)) p_i q_t^\top \right\|_2 \leq \sqrt{\frac{K \log(\frac{d_1+d_2}{\delta})}{n}} S_2^2 =: \epsilon(n, \delta),$$

with probability at least $1 - \delta$.

Plugging in the results of Lemma 5 and 6 to Lemma 4, we have the following result on the converged estimator $\hat{\Phi}$:

Lemma 7. If $\|\Phi_0 - \Phi^*\| \leq c_2 \sqrt{\sigma_r}$ where $c_2 \leq \sqrt{\min\{\mu, 2\} \cdot (6L + 4)}$, then:

$$\|\hat{\Phi} - \Phi^*\|_F^2 \leq \frac{288\sigma_1^2}{\sigma_r \cdot \kappa} \cdot \left(\frac{3}{4} + \frac{8n}{\kappa \lambda_{\min}(V_n)} + \frac{n}{\lambda_{\max}(V_n)} \right) \frac{K r \log(\frac{d_1+d_2}{\delta})}{\lambda_{\min}(V_n)} S_2^4.$$

Now it remains to establish a bound on $\lambda_{\min}(V_n)$ and $\lambda_{\max}(V_n) = \|V_n\|_2$.

Lemma 8. If

$$n \geq 4\sigma^2(C_1 \sqrt{d_1 d_2} + C_2 \sqrt{\log(1/\delta)})^2 + \frac{2B}{\lambda_{\min}(\Sigma)K},$$

for some fixed constant C_1, C_2 , with probability at least $1 - \delta$ we have $\lambda_{\min}(V_n) \geq B$ and

$$\frac{\|V_n\|_2}{n} \geq \frac{1}{2} K \|\Sigma\|_2.$$

Combining Lemma 7 and Lemma 8, we have Proposition 1. In the remaining part of the section, we provide proof of the Lemmas.

S.7.2.2 Proof of Lemma 5

For proof of Lemma 5, we use Taylor expansion and bounds on the second moment of the loss function. From the definition of the loss function, We can easily check that

$$\nabla^2 \mathcal{L}_n(\phi) = \frac{1}{n} \sum_{t=1}^n \left[\sum_{i \in S_t} p_t(i|\phi) x_{it} x_{it}^\top - \sum_{i \in S_t} \sum_{j \in S_t} p_t(i|\phi) p_t(j|\phi) x_{it} x_{jt}^\top \right].$$

Also note that from Taylor expansion we have:

$$\mathcal{L}_n(Y) - \mathcal{L}_n(X) - \langle \nabla \mathcal{L}_n(X), Y - X \rangle = (y - x)^\top \nabla^2 \mathcal{L}_n(\bar{\phi})(y - x), \quad (\text{S3})$$

where $x = \text{vec}(X)$, $y = \text{vec}(Y)$, $\bar{\phi} = cx + (1 - c)y$ for some $c \in (0, 1)$. Also note that for any vector a, b , $(a - b)(a - b)^\top \succeq 0$ and therefore:

$$aa^\top + bb^\top \succeq ab^\top + ba^\top. \quad (\text{S4})$$

Using this fact we have:

$$\begin{aligned} & \sum_{i \in S_t} p_t(i|\phi) x_{it} x_{it}^\top - \sum_{i \in S_t} \sum_{j \in S_t} p_t(i|\phi) p_t(j|\phi) x_{it} x_{jt}^\top \\ &= \sum_{i \in S_t} p_t(i|\phi) x_{it} x_{it}^\top - \frac{1}{2} \sum_{i \in S_t} \sum_{j \in S_t} p_t(i|\phi) p_t(j|\phi) (x_{it} x_{jt}^\top + x_{jt} x_{it}^\top) \\ &\succeq \sum_{i \in S_t} p_t(i|\phi) x_{it} x_{it}^\top - \frac{1}{2} \sum_{i \in S_t} \sum_{j \in S_t} p_t(i|\phi) p_t(j|\phi) (x_{it} x_{it}^\top + x_{jt} x_{jt}^\top) \quad (\because (\text{S4})) \\ &= \sum_{i \in S_t} p_t(i|\phi) x_{it} x_{it}^\top - \sum_{i \in S_t} \sum_{j \in S_t} p_t(i|\phi) p_t(j|\phi) x_{it} x_{it}^\top \\ &= \sum_{i \in S_t} p_t(i|\phi) p_t(0|\phi) x_{it} x_{it}^\top. \quad \left(\because 1 - \sum_{j \in S_t} p_t(j|\phi) = p_t(0|\phi) \right) \end{aligned}$$

Now assume $\bar{\phi} \in \mathcal{B}(\phi^*, 1)$, and suppose $p_t(i|\phi)p_t(0|\phi) \geq \kappa$ for every t and $\phi \in \mathcal{B}(\phi^*, 1)$. Applying the inequality above to (S3), we have:

$$\begin{aligned} & (y - x)^\top \nabla^2 \mathcal{L}_n(\bar{\phi})(y - x) \\ & \geq (y - x)^\top \left(\frac{1}{n} \sum_{t=1}^n \sum_{i \in S_t} p_t(i|\bar{\phi}) p_t(0|\bar{\phi}) x_{it} x_{it}^\top \right) (y - x) \\ & \geq (y - x)^\top \frac{\kappa}{n} V_n (y - x) \quad \left(\because V_n = \sum_{t=1}^n \sum_{i \in S_t} x_{it} x_{it}^\top \right) \\ & \geq \frac{\kappa}{n} \lambda_{\min}(V_n) \|y - x\|^2 \\ & = \frac{\kappa}{n} \lambda_{\min}(V_n) \|Y - X\|_F^2, \quad (\because \text{vec}(X) = x, \text{vec}(Y) = y) \end{aligned}$$

which gives the left side of the inequality. Now also consider that:

$$\begin{aligned}
& \sum_{i \in S_t} p_t(i|\phi) x_{it} x_{it}^\top - \sum_{i \in S_t} \sum_{j \in S_t} p_t(i|\phi) p_t(j|\phi) x_{it} x_{jt}^\top \\
&= \sum_{i \in S_t} p_t(i|\phi) x_{it} x_{it}^\top - \left(\sum_{i \in S_t} p_t(i|\phi) x_{it} \right) \left(\sum_{i \in S_t} p_t(i|\phi) x_{it} \right)^\top \\
&\preceq \sum_{i \in S_t} p_t(i|\phi) x_{it} x_{it}^\top \\
&\preceq \sum_{i \in S_t} x_{it} x_{it}^\top. \quad (\because p_t(i|\phi) \leq 1)
\end{aligned}$$

Applying the inequality to (S3), we have:

$$\begin{aligned}
(y - x)^\top \nabla^2 \mathcal{L}_n(\bar{\phi})(y - x) &\leq (y - x)^\top \left(\frac{1}{n} \sum_{t=1}^n \sum_{i \in S_t} x_{it} x_{it}^\top \right) (y - x) \\
&= \frac{1}{n} (y - x)^\top V_n (y - x) \\
&\leq \frac{1}{n} \lambda_{\max}(V_n) \|Y - X\|_F^2,
\end{aligned}$$

which completes the proof.

S.7.2.3 Proof of Lemma 6

We use the following Bernstein inequality for rectangular matrices from (Tropp, 2012):

Lemma 9 ((Bernstein Inequality for Rectangular Matrices, Theorem 1.6 of (Tropp, 2012)). *Suppose $Z_k \in \mathbb{R}^{d_1 \times d_2}$ are independent random matrices. Suppose $\mathbb{E} Z_k = 0$ and $\|Z_k\|_2 \leq R$ almost surely.*

Define

$$\sigma^2 := \max \left\{ \left\| \sum_k \mathbb{E}(Z_k Z_k^\top) \right\|, \left\| \sum_k \mathbb{E}(Z_k^\top Z_k) \right\| \right\}.$$

Then for all $t \geq 0$,

$$\mathbb{P} \left\{ \left\| \sum_k Z_k \right\| \geq t \right\} \leq (d_1 + d_2) \cdot \exp \left(\frac{-t^2/2}{\sigma^2 + Rt/3} \right).$$

Let us plug in $Z_t = \sum_{i \in S_t} (y_{it} - p_t(i|\Phi^*)) p_i q_t^\top$ to apply Lemma 9. For brevity, let us denote

$\epsilon_{it} = y_{it} - p_t(i|\Phi^*)$. We can easily check that $\mathbb{E} \epsilon_{it} = 0$.

Now to verify R in the conditions of Lemma 9, note that $Z_t = \sum_{i \in S_t} \epsilon_{it} p_i q_t^\top$, therefore $\mathbb{E} Z_t = 0$.

Now note that $\|p_i\|, \|q_t\| \leq S_2$ for every $i \in [N]$ and $t \in [T]$. Note that

$$\|p_i q_t^\top v\| = q_t^\top v \|p_i\| \leq \|q_t\| \cdot \|v\| \cdot \|p_i\| \leq S_2^2 \|v\|.$$

Therefore $\|p_i q_t^\top\|_2 \leq S_2^2$. Now let $i(t)$ be the item selected for user t , where $i(t) = 0$ if no items were selected. Also let $\epsilon_{0t} = 0$. Note that $1 \geq \epsilon_{i(t)t} \geq 0$ and $\epsilon_{jt} \leq 0$ for $j \neq i(t)$ and moreover $0 \geq \sum_{S(t) \setminus \{i(t)\}} \epsilon_{jt} \geq -1$. Therefore,

$$\begin{aligned} \|Z_t\|_2 &= \left\| \sum_{i \in S_t} \epsilon_{it} \cdot p_i q_t^\top \right\|_2 \\ &\leq \epsilon_{i(t),t} \cdot \|p_{i(t)} q_t^\top\|_2 + \sum_{S(t) \setminus \{i(t)\}} (-\epsilon_{jt}) \cdot \|p_i q_t^\top\|_2 \\ &\leq \epsilon_{i(t),t} S_2^2 + \sum_{S(t) \setminus \{i(t)\}} (-\epsilon_{jt}) \cdot S_2^2 \\ &\leq 2S_2^2, \end{aligned}$$

which allows us to write $R = 2S_2^2$. Next we verify σ^2 . Note that:

$$\begin{aligned} \sum_{t=1}^n \mathbb{E} Z_t Z_t^\top &= \mathbb{E} \left[\sum_{t=1}^n \sum_{i \in S_t} \epsilon_{it}^2 \cdot p_i q_t^\top q_t p_i^\top \right] \\ &= \sum_{t=1}^n \sum_{i \in S_t} \mathbb{E} \epsilon_{it}^2 p_i q_t^\top q_t p_i^\top \\ &= \sum_{t=1}^n \sum_{i \in S_t} p_t(i|\Phi^*) (1 - p_t(i|\Phi^*)) p_i q_t^\top q_t p_i^\top, \end{aligned}$$

since $\mathbb{E} \epsilon_{it}^2 = \text{Var}(\epsilon_{it}) = \text{Var}(y_{it}) = (\mathbb{E} y_{it})(1 - \mathbb{E} y_{it})$. Also note that $\|p p^\top v\| = |p^\top v| \cdot \|p\| \leq \|p\|^2 \cdot \|v\|$, so $\|p p^\top\|_2 = \|p\|^2$. Therefore,

$$\left\| \sum_{t=1}^n \mathbb{E} Z_t Z_t^\top \right\|_2 = \left\| \sum_{t=1}^n \sum_{i \in S_t} p_t(i|\Phi^*) (1 - p_t(i|\Phi^*)) (q_t^\top q_t) p_i p_i^\top \right\|_2$$

$$\begin{aligned}
&\leq \sum_{t=1}^n \sum_{i \in S_t} p_t(i|\Phi^*) (1 - p_t(i|\Phi^*)) \|q_t\|_2^2 \|p_i p_i^\top\|_2 \\
&\leq \frac{1}{4} \sum_{t=1}^n \sum_{i \in S_t} \|p_i\|_2^2 \|q_t\|_2^2 \quad (\because p(1-p) \leq 1/4) \\
&\leq \frac{nK}{4} S_2^4. \quad (\because \|p_i\|_2, \|q_t\|_2 \leq S_2)
\end{aligned}$$

and similarly we have:

$$\left\| \sum_{t=1}^n \mathbb{E} Z_t^\top Z_t \right\|_2 \leq \frac{nK}{4} S_2^4.$$

Now applying the Lemma 9 with $R = 2S_2^2$ and $\sigma^2 = \frac{nK}{4} S_2^4$ we have:

$$\mathbb{P} \left(\left\| \frac{1}{n} \sum_{t=1}^n Z_t \right\|_2 \geq t \right) \leq (d_1 + d_2) \exp \left(- \frac{6nt^2}{S_2^2(3KS_2^2 + 8t)} \right).$$

Let $\eta = \log \frac{d_1 + d_2}{\delta}$ for some $\delta \in (0, 1)$. Assuming $n \geq \frac{64}{9} K \eta^2$, we have $\frac{3}{8} K S_2^2 \geq \sqrt{\frac{K\eta}{n}} S_2^2$. Now select $t = \sqrt{\frac{K\eta}{n}} S_2^2 \leq \frac{3}{8} K S_2^2$. Then we have $8t \leq 3KS_2^2$ and $nt^2 \geq K\eta S_2^4$. Therefore we have

$$\begin{aligned}
\mathbb{P} \left(\left\| \frac{1}{n} \sum_{t=1}^n Z_t \right\|_2 \geq t \right) &\leq (d_1 + d_2) \exp \left(- \frac{6nt^2}{S_2^2(3KS_2^2 + 8t)} \right) \\
&\leq (d_1 + d_2) \exp(-\eta) = \delta.
\end{aligned}$$

Therefore,

$$\left\| \frac{1}{n} \sum_{t=1}^n \sum_{i \in S_t} (y_{it} - p_t(i|\Phi^*)) p_i q_t^\top \right\|_2 \leq \sqrt{\frac{K \log(\frac{d_1 + d_2}{\delta})}{n}} S_2^2 = \epsilon(n, \delta),$$

with probability at least $1 - \delta$. This completes the proof of Lemma 6.

S.7.2.4 Proof of Lemma 7

Before moving on to the main proof of Lemma 7, we first state the modified result from (Wang et al., 2017) and Lemma 4.

Proposition 4. For $i = 1, 2$, let $U_i \in \mathbb{R}^{d_1 \times r}$, $V_i \in \mathbb{R}^{d_2 \times r}$ and $X_i = U_i V_i^\top$. Now denote

$$Z_1 = \begin{pmatrix} U_1 \\ V_1 \end{pmatrix}, \quad Z_2 = \begin{pmatrix} U_2 \\ V_2 \end{pmatrix}.$$

Then,

$$\|X_1 - X_2\|_F^2 \leq 2(\|Z_2\|_2 + d(Z_1, Z_2))^2 d^2(Z_1, Z_2).$$

Proof. Note that for two positive definite matrices A, B with eigenvalue decomposition $A = P\Lambda P^\top$ and $B = QDQ^\top$,

$$\begin{aligned} \text{tr}(AB) &= \text{tr}(P\Lambda P^\top QDQ^\top) \\ &= \text{tr}(Q^\top P\Lambda P^\top QD) \quad (\because \text{tr}(AB) = \text{tr}(BA)) \\ &\leq \text{tr}(Q^\top P\Lambda P^\top Q) \cdot \|D\|_2 \quad (\because \text{tr}(AB) \leq \text{tr}(A) \cdot \|B\|_2) \\ &= \text{tr}(\Lambda) \cdot \|D\|_2 \\ &= \text{tr}(A) \cdot \|B\|_2. \end{aligned}$$

This implies:

$$\begin{aligned} \|AB\|_F^2 &= \text{tr}(ABB^\top A^\top) \\ &= \text{tr}(BB^\top A^\top A) \\ &\leq \text{tr}(BB^\top) \|A^\top A\|_2 \\ &= \|B\|_F^2 \|A\|_2^2 \end{aligned}$$

and therefore $\|AB\|_F \leq \|B\|_F \|A\|_2$. Now consider $R \in \mathbb{Q}_r$. Note that:

$$\begin{aligned} \|U_1(V_1 - V_2R)^\top\|_F^2 &= \text{tr}(U_1(V_1 - V_2R)^\top(V_1 - V_2R)U_1^\top) \\ &= \text{tr}((V_1 - V_2R)^\top(V_1 - V_2R)U_1^\top U_1) \\ &\leq \|U_1^\top U_1\|_2 \cdot \text{tr}((V_1 - V_2R)^\top(V_1 - V_2R)) \end{aligned}$$

$$= \|U_1\|_2^2 \|V_1 - V_2 R\|_F^2.$$

Similarly we have $\|(U_1 - U_2 R)R^\top V_2^\top\|_F^2 \leq \|V_2\|_2^2 \|U_1 - U_2 R\|_F^2$. Now note that for arbitrary vector v ,

$$\|Z_i v\|_2^2 = \|U_i v\|_2^2 + \|V_i v\|_2^2 \geq \|U_i v\|_2^2.$$

So we have $\|Z_i\|_2 \geq \|U_i\|_2$ and similarly $\|Z_i\|_2 \geq \|V_i\|_2$. Now note that:

$$\begin{aligned} \|Z_1\|_2 &\leq \|Z_1 - Z_2 R\|_2 + \|Z_2 R\|_2 \\ &= \|Z_1 - Z_2 R\|_2 + \|Z_2\|_2 \quad (\because R \in \mathbb{Q}_r) \\ &\leq \|Z_1 - Z_2 R\|_F + \|Z_2\|_2. \quad (\because \|A\|_2 \leq \|A\|_F) \end{aligned}$$

And this holds for arbitrary $R \in \mathbb{Q}_r$. Therefore,

$$\|Z_1\|_2 \leq \|Z_2\|_2 + d(Z_1, Z_2). \quad (\text{S5})$$

And as $(a+b)^2 \leq a^2 + b^2$, we have $\|Z_1\|_2^2 \leq 2(\|Z_2\|_2^2 + d(Z_1, Z_2))$. Therefore we have:

$$\begin{aligned} \|X_1 - X_2\|_F^2 &= \|U_1 V_1^\top - U_2 V_2^\top\|_F^2 \\ &= \|U_1 V_1^\top - U_1 R^\top V_2^\top + U_1 R^\top V_2^\top - U_2 R R^\top V_2^\top\|_F^2 \\ &\leq (\|U_1(V_1 - V_2 R)^\top\|_F + \|(U_1 - U_2 R)R^\top V_2^\top\|_F)^2 \\ &\leq 2(\|U_1(V_1 - V_2 R)^\top\|_F^2 + \|(U_1 - U_2 R)R^\top V_2^\top\|_F^2) \quad (\because (a+b)^2 \leq 2(a^2 + b^2)) \\ &\leq 2(\|V_2\|_2^2 \|U_1 - U_2 R\|_F^2 + \|U_1\|_2^2 \|V_1 - V_2 R\|_F^2) \quad (\because \|AB\|_F^2 \leq \|A\|_F \|B\|_2) \\ &\leq 2(\|Z_2\|_2^2 \|U_1 - U_2 R\|_F^2 + \|Z_1\|_2^2 \|V_1 - V_2 R\|_F^2) \\ &\leq 2(\|Z_2\|_2 + d(Z_1, Z_2))^2 (\|U_1 - U_2 R\|_F^2 + \|V_1 - V_2 R\|_F^2) \quad (\because (\text{S5})) \\ &= 2(\|Z_2\|_2 + d(Z_1, Z_2))^2 \|Z_1 - Z_2 R\|_F^2. \end{aligned}$$

Since this holds for arbitrary $R \in \mathbb{Q}_r$, The statement holds. \square

Now we can finally prove Lemma 7.

Proof. Assume $d(Z^{(0)}, Z^*) \leq \kappa_1$ and $C_1\epsilon(n, \delta) \leq (1 - \rho)\kappa_1$. Then by induction and using 4, we can check that $d(Z^{(t)}, Z^*) \leq \kappa_1$ for every $t \geq 0$. Also we have:

$$\begin{aligned} d^2(Z^{(t)}, Z^*) &\leq \rho^t d^2(Z^{(0)}, Z^*) + \frac{C_1(1 - \rho^t)}{1 - \rho} \epsilon^2(n, \delta) \\ &\leq \rho^t \kappa_1^2 + \frac{C_1}{1 - \rho} \epsilon^2(n, \delta). \end{aligned}$$

Note that $\|Z^*\|_2 \leq 2\|\Phi^*\|_2 = 2\sigma_1$. Using Proposition 4, we have:

$$\begin{aligned} \|\Phi^{(t)} - \Phi^*\|_F^2 &\leq 2(2\sigma_1 + d(Z^{(t)}, Z^*))^2 d^2(Z^{(t)}, Z^*) \\ &\leq (8\sigma_1^2 + 2d^2(Z^{(t)}, Z^*)) d^2(Z^{(t)}, Z^*). \quad (\because (a + b)^2 \leq 2(a^2 + b^2)) \end{aligned}$$

As $t \rightarrow \infty$, we have:

$$\|\hat{\Phi} - \Phi^*\|_F^2 \leq \left(8\sigma_1^2 + \frac{2C_1}{1 - \rho} \epsilon^2(n, \delta)\right) \cdot \frac{C_1}{1 - \rho} \epsilon^2(n, \delta).$$

Now assume $\epsilon^2(n, \delta) \leq \frac{(1 - \rho)\sigma_1^2}{2C_1}$. Then we have:

$$\|\hat{\Phi} - \Phi^*\|_F^2 \leq \frac{9\sigma_1^2 C_1}{1 - \rho} \epsilon^2(n, \delta).$$

Now note that $C_1 = r(48\delta^2\sigma_1 + 2\delta(8/\mu + 1/L))$. So we have:

$$\|\hat{\Phi} - \Phi^*\|_F^2 \leq \frac{9\sigma_1^2}{1 - \rho} \left(48\delta^2\sigma_1 + 2\delta \left(\frac{8}{\mu} + \frac{1}{L}\right)\right) r\epsilon^2(n, \delta).$$

Plugging in the values of $\delta = c/\sigma_1$ and $\rho = 1 - \delta\mu\sigma_4/16$ we have:

$$\|\hat{\Phi} - \Phi^*\|_F^2 \leq 9\sigma_1^2 \cdot \frac{32}{\mu\sigma_r} \left(24c_1 + \frac{8}{\mu} + \frac{1}{L}\right) r\epsilon^2(n, \delta).$$

Now note that the constants are defined as:

$$\mu = \frac{\kappa}{n} \lambda_{\min}(V_n)$$

$$\begin{aligned}
L &= \frac{1}{n} \lambda_{\max}(V_n) \\
\epsilon(n, \delta) &= \sqrt{\frac{K \log(\frac{d_1+d_2}{\delta})}{n}} S_2^2 \\
c_1 &\leq \min\left(\frac{1}{32}, \frac{\mu}{192L^2}\right) \leq \frac{1}{32}.
\end{aligned}$$

Plugging in the values we achieve:

$$\begin{aligned}
\|\hat{\Phi} - \Phi^*\|_F^2 &\leq \frac{288\sigma_1^2}{\sigma_r} \cdot \frac{n}{\kappa\lambda_{\min}(V_n)} \cdot \left(24c_1 + \frac{8n}{\kappa\lambda_{\min}(V_n)} + \frac{n}{\lambda_{\max}(V_n)}\right) r \cdot \frac{K \log(\frac{d_1+d_2}{\delta})}{n} S_2^4 \\
&= \frac{288\sigma_1^2}{\sigma_r \cdot \kappa} \cdot \left(\frac{3}{4} + \frac{8n}{\kappa\lambda_{\min}(V_n)} + \frac{n}{\lambda_{\max}(V_n)}\right) \frac{Kr \log(\frac{d_1+d_2}{\delta})}{\lambda_{\min}(V_n)} S_2^4,
\end{aligned}$$

which completes the proof. \square

S.7.2.5 Proof of Lemma 8

For proof of Lemma 8, we modify results from Vershynin (2010) about concentration inequalities of random matrices with sub-gaussian rows.

Note that from Assumption 1, q_t are i.i.d. where $\mathbb{E}[q_t q_t^\top] = \Sigma_q$. Also note that S_t are uniformly sampled from $[N]$ with size K in the exploration stage, where S_t 's and q_t 's are independent. As S_t are sampled uniformly, we have $\mathbb{E} \sum_{i \in S_t} p_i p_i^\top = \frac{K}{N} \sum_{i=1}^N p_i p_i^\top =: K \Sigma_p$. Now note that:

$$\mathbb{E} \left[\sum_{t=1}^n \sum_{i \in S_t} x_{it} x_{it}^\top \right] = n K \Sigma_q \otimes \Sigma_p =: n K \Sigma.$$

Define $a_{it} = \Sigma^{-1/2} x_{it}$. Consider the matrix $A \in \mathbb{R}^{nK \times d_1 d_2}$ with a_{it} as its rows. Note that $A^\top A = \sum_t \sum_i a_{it} a_{it}^\top = \Sigma^{-1/2} V_n \Sigma^{-1/2}$. Instead of analyzing V_n directly, we first claim the following concentration inequality:

$$\left\| \frac{1}{nK} A^\top A - I \right\| \leq \max(\delta, \delta^2) =: \epsilon.$$

We use the following lemma from Vershynin (2010).

Lemma 10 (Lemma 5.4 of Vershynin (2010)). *Let A be a symmetric $n \times n$ matrix and let \mathcal{N}_ϵ be an ϵ -net of S^{n-1} for some $\epsilon \in [0, 1]$. Then,*

$$\|A\| = \sup_{x \in S^{n-1}} |\langle Ax, x \rangle| \leq (1 - 2\epsilon)^{-1} \sup_{x \in \mathcal{N}_\epsilon} |\langle Ax, x \rangle|.$$

Applying this lemma, it suffices to show

$$\max_{v \in \mathcal{N}} \left| \frac{1}{NK} \|Av\|_2^2 - 1 \right| \leq \frac{\epsilon}{2},$$

where \mathcal{N} is the $\frac{1}{4}$ -net of sphere $S^{d_1 d_2 - 1}$. Now note that

$$\begin{aligned} \|Av\|_2^2 &= \sum_{t=1}^n \sum_{i \in S_t} (a_{it}^\top v)^2 \\ &= \sum_{t=1}^n \sum_{i \in S_t} \left(x_{it} \Sigma^{-1/2} v \right)^2 && (\because \text{Definition of } a_{it}) \\ &= \sum_{t=1}^n \sum_{i \in S_t} \langle p_i q_t^\top, U \rangle^2 \\ &= \sum_{t=1}^n \sum_{i \in S_t} (p_i^\top U q_t)^2, \end{aligned}$$

where $U \in \mathbb{R}^{d_2 \times d_1}$ with $\text{vec}(U) = \Sigma^{-1/2} v$. Now note that:

$$\text{vec}(U) = \Sigma^{-1/2} v = (\Sigma_q^{-1/2} \otimes \Sigma_p^{-1/2}) v = \text{vec}(\Sigma_p^{-1/2} V \Sigma_q^{-1/2}),$$

where $\text{vec}(V) = v$. Therefore:

$$p_i^\top U q_t = \left(\Sigma_p^{-1/2} p_i \right)^\top V \left(\Sigma_q^{-1/2} q_t \right) = x_i^\top V y_t.$$

To show this we first show that these sums are actually sub-exponential random variables. Suppose y_t 's are sub-Gaussian random vector with $\|y_t\|_{\psi_2} \leq \sigma$. For $p \geq 1$ and $v \in S^{d_1-1}$, $\|v^\top y_t\|_{\psi_2} \leq \|y_t\|_{\psi_2} \leq \sigma$. Note that $2p \geq 1$. By definition of $\|\cdot\|_{\psi_2}$, we have $(\mathbb{E} \|v^\top y_t\|^{2p})^{1/2p} / \sqrt{2p} \leq \sigma$ which gives

$$\frac{(\mathbb{E} \|v^\top y_t\|^{2p})^{1/p}}{p} \leq 2\sigma^2 \tag{S6}$$

Also fix $S \subset [N]$ as a set of size K independent of u . Moreover assume that $\max_{i \in [N]} \|x_i\| \leq S_v < \infty$ and note that $\|v\|_2^2 = \|V\|_F^2 = 1$ as $v \in \mathcal{N}$. Then,

$$\begin{aligned}
\sup_{p \geq 1} \frac{(\mathbb{E} [\sum_{i \in S} (x_i^\top V y_t)^2]^p)^{1/p}}{p} &\leq \sup_{p \geq 1} \frac{(\mathbb{E} \frac{K^p}{K} \sum_{i \in S} (x_i^\top V y_t)^{2p})^{1/p}}{p} && (\because \text{Jensen's Inequality}) \\
&\leq K \sup_{p \geq 1} \frac{(\sum_{i \in S} \mathbb{E} [x_i^\top V y_t]^{2p})^{1/p}}{p} && (\because K \geq 1) \\
&\leq K \sup_{p \geq 1} \frac{\sum_{i \in S} (\mathbb{E} [x_i^\top V y_t]^{2p})^{1/p}}{p} \\
&\leq K \sum_{i \in S} \sup_{p \geq 1} \frac{(\mathbb{E} [x_i^\top V y_t]^{2p})^{1/p}}{p} \\
&\leq K \sup_{p \geq 1} \left(\mathbb{E} \left[\sum_{i \in S} 2\sigma^2 \cdot \|V^\top x_i\|_2^2 \right]^p \right)^{1/p} && (\because (S6)) \\
&= 2\sigma^2 K \sup_{p \geq 1} \left(\mathbb{E} \left[\sum_{i \in S} \|V^\top x_i\|_2^2 \right]^p \right)^{1/p} \\
&\leq 2\sigma^2 K \cdot \max_S \sum_{i \in S} \|V^\top x_i\|_2^2 \\
&\leq 2\sigma^2 K^2 S_v^2 \|V\|_2^2 \\
&\leq 2\sigma^2 K^2 S_v^2 \|V\|_F^2 \\
&\leq 2\sigma^2 K^2 S_v^2.
\end{aligned}$$

Therefore $Z_t = \sum_{i \in S} (x_i^\top V y_t)^2$ is sub-exponential with parameter $2\sigma^2 K^2 S_v^2$. Therefore, from Remark 5.18 from Vershynin (2010), centered Z_t , i.e., $Z_t - K$ are independent centered sub-exponential variables with parameter $4\sigma^2 K^2 S_v^2$. Now consider the following result for centered sub-exponential random variables:

Lemma 11 (Corollary 5.17 of (Vershynin, 2010)). *Let X_1, \dots, X_N be independent centered sub-exponential random variables, and let $K = \max_i \|X_i\|_{\psi_1}$. Then, for every $\epsilon \geq 0$, we have*

$$\mathbb{P} \left\{ \left| \sum_{i=1}^N X_i \right| \geq \epsilon N \right\} \leq 2 \exp \left[-c \min \left(\frac{\epsilon^2}{K^2}, \frac{\epsilon}{K} \right) N \right].$$

Using exponential deviation inequality, and assuming $8\sigma^2 S_v^2 \geq 1$, we have:

$$\begin{aligned}
\mathbb{P} \left(\left| \frac{1}{nK} \|Av\|_2^2 - 1 \right| \geq \frac{\epsilon}{2} \right) &= \mathbb{P} \left(\left| \frac{1}{n} \sum_{i=1}^n (Z_t - K) \right| \geq \frac{K\epsilon}{2} \right) \\
&\leq 2 \exp \left[-c \left(\left(\frac{K\epsilon}{8\sigma^2 K^2 S_v^2} \right)^2 \wedge \left(\frac{K\epsilon}{8\sigma^2 K^2 S_v^2} \right) \right) n \right] \\
&\leq 2 \exp \left[-\frac{c}{64\sigma^2 K^2 S_v^4} (\epsilon^2 \wedge 8\sigma^2 S_v^2 \epsilon) n \right] \\
&\leq 2 \exp \left[-\frac{c}{64\sigma^2 K^2 S_v^4} (\epsilon^2 \wedge \epsilon) n \right] \\
&= 2 \exp \left[-\frac{c}{64\sigma^2 K^2 S_v^4} \delta^2 n \right] \\
&\leq 2 \exp \left[-\frac{c}{64\sigma^2 K^2 S_v^4} (C^2 d_1 d_2 + t^2) \right],
\end{aligned}$$

where $\epsilon = \max(\delta, \delta^2)$ and $\delta = C\sqrt{\frac{d_1 d_2}{n}} + \frac{t}{\sqrt{n}}$. Now consider the following lemma about covering number of the sphere.

Lemma 12 (Lemma 5.2 of (Vershynin, 2010)). *The unit Euclidean sphere S^{n-1} equipped with the Euclidean metric satisfies for every $\epsilon < 0$ that*

$$\mathcal{N}(S^{n-1}, \epsilon) \leq \left(1 + \frac{2}{\epsilon} \right)^n.$$

Then we have $|\mathcal{N}| \leq 9^{d_1 d_2}$. Considering the union bound:

$$\begin{aligned}
\mathbb{P} \left(\max_{v \in \mathcal{N}} \left| \frac{1}{nK} \|Av\|_2^2 - 1 \right| \leq \frac{\epsilon}{2} \right) &\leq 9^{d_1 d_2} \cdot 2 \exp \left[-\frac{c}{64\sigma^2 K^2 S_v^4} (C^2 d_1 d_2 + t^2) \right] \\
&\leq 2 \exp(-c_1 t^2),
\end{aligned}$$

for $C \geq 8\sigma K S_v^2 \sqrt{\log 9/c}$ and $c_1 = c/(64\sigma^2 K^2 S_v^4)$. So we have with probability $1 - 2 \exp(-c_1 t^2)$,

$$\left\| \frac{1}{nK} A^\top A - I \right\| \leq \max(\delta, \delta^2).$$

Now note that for a non-negative matrix M , if $\|M - I\|_2 \leq \epsilon$, then for arbitrary v such that

$$\|v\| = 1,$$

$$\|Mv\| \geq \|v\| - \|(M - I)v\| \geq 1 - \epsilon.$$

Therefore $\lambda_{\min}(M) \geq 1 - \epsilon$. Now assume $\delta \leq 1$, then we have with probability $1 - 2 \exp(-c_1 t^2)$,

$$\lambda_{\min}(A^\top A) \geq nK - nK \left(C \sqrt{\frac{d_1 d_2}{n}} + \frac{t}{\sqrt{n}} \right) = nK - K\sqrt{n}(C\sqrt{d_1 d_2} + t).$$

Note that $A^\top A = \Sigma^{-1/2} V_n \Sigma^{-1/2}$. Therefore,

$$\lambda_{\min}(V_n) \geq \lambda_{\min}(\Sigma) nK - \lambda_{\min}(\Sigma) K\sqrt{n}(C\sqrt{d_1 d_2} + t),$$

and similarly:

$$\|V_n\| \geq \|\Sigma\|_2(nK - K\sqrt{n}(C\sqrt{d_1 d_2} + t)).$$

Note that if $n \geq (2b/a)^2 + 2B/a$,

$$\begin{aligned} an - b\sqrt{n} &\geq \frac{an}{2} + a \left(\frac{n}{2} - \frac{b}{a}\sqrt{n} \right) \\ &\geq \frac{a}{2} \cdot n + \frac{a\sqrt{n}}{2} \left(\sqrt{n} - \frac{2b}{a} \right) \\ &\geq B. \end{aligned}$$

Therefore, if

$$n \geq 4\sigma^2(C_1\sqrt{d_1 d_2} + C_2\sqrt{\log(1/\delta)})^2 + \frac{2B}{\lambda_{\min}(\Sigma)K},$$

for constants C_1, C_2 defined as $C_1 = 4KS_v^2\sqrt{\log 9/c}$ and $C_2 = 8KS_v^2/\sqrt{c}$, then with probability at least $1 - \delta$ we have $\lambda_{\min}(V_n) \geq B$.

Also note that

$$\begin{aligned} \frac{1}{nK} \|V_n\|_2 &= \|\Sigma^{1/2} \frac{1}{nK} A^\top A \Sigma^{1/2}\|_2 \\ &\geq \|\Sigma^{1/2} I \Sigma^{1/2}\|_2 - \|\Sigma^{1/2} \left(\frac{1}{nK} A^\top A - I \right) \Sigma^{1/2}\|_2 \\ &\geq \|\Sigma\|_2 - \|\Sigma^{1/2}\|_2 \cdot \left\| \frac{1}{nK} A^\top A - I \right\|_2 \|\Sigma^{1/2}\|_2 \\ &\geq \|\Sigma\|_2(1 - \epsilon). \end{aligned}$$

Therefore,

$$\frac{\|V_n\|_2}{n} \geq K\|\Sigma\|_2 \left(1 - \frac{1}{\sqrt{n}}(C_1\sqrt{d_1d_2} + C_2\sqrt{\log(1/\delta)})\right).$$

Assuming $n \geq 4(C_1\sqrt{d_1d_2} + C_2\log(1/\delta))^2$, we have

$$\frac{\|V_n\|_2}{n} \geq \frac{1}{2}K\|\Sigma\|_2.$$

S.7.3 Proof of Proposition 3

Proposition 3 provides bounds on the error induced by truncation. We begin with the following Lemma from Jun et al. (2019).

Lemma 13 (Wedin's $\sin\Theta$ theorem, Appendix B of (Jun et al., 2019)). *Let $\hat{\Theta} = [\hat{U}, \hat{U}_\perp]\hat{D}[\hat{V}, \hat{V}_\perp]^\top$ and $\Theta^* = U^*D^*V^*$ be the SVD of $\hat{\Theta}$ and Θ^* . Then,*

$$\|\hat{U}_\perp^\top U^*\|_F \|\hat{V}_\perp^\top V^*\|_F \leq \frac{\|\hat{\Theta} - \Theta^*\|_F^2}{s_r^{*2}},$$

where s_k^* is the k -th (smallest) eigenvalue of Θ^* .

Now let θ^* be the rotation-vectorization of $[\hat{U}, \hat{U}_\perp]^\top \Phi^*[\hat{V}, \hat{V}_\perp]$. Then we have

$$\|\theta_{k+1:p}^*\|_2 \leq \|\hat{U}_\perp U\|_F \|\hat{V}_\perp V\|_F \cdot \|D^*\|_2 \leq \frac{s_1^*}{s_r^{*2}} \|\hat{\phi} - \phi^*\|^2.$$

Combining Proposition 1 and Lemma 13, the proof is complete.

S.7.4 Proof of Theorem 1

Theorem 1 provides bounds on the cumulative regret of our proposed algorithm. In this section we provide a more detailed proof of the theorem. First we restate the following result from Oh and Iyengar (2021).

Lemma 14 (Lemma 6 from Oh and Iyengar (2021)). *If $\lambda_{\min}(W_{T_0}) \geq K$, then*

$$\sum_{t=1}^T \max_{i \in S_t} \|x_{it,rtv}\|_{W_t^{-1}}^2 \leq 2k \log(T/k).$$

Now define the event $\mathcal{E}_t := \{\|\hat{\theta}_{n,rtv} - \theta_{rtv}^*\| \leq \alpha_n\}$. Then conditioned on \mathcal{E}_t , we have:

$$\begin{aligned} r_t &= R(\{\langle X_{it}, \Theta^* \rangle\}, S^*) - R(\{\langle X_{it}, \Theta^* \rangle\}, S_t) \\ &\leq R(\{z_{it}\}, S^*) - R(\{\langle X_{it}, \Theta^* \rangle\}, S_t) \\ &\leq R(\{z_{it}\}, S_t) - R(\{\langle X_{it}, \Theta^* \rangle\}, S_t) \\ &\leq R_{\max} \cdot \max_{i \in S_t} (z_{it} - \langle X_{it}, \Theta^* \rangle) \\ &\leq R_{\max} \cdot 2\alpha_t \max_{i \in S_t} \|x_{it,rtv}\|_{W_t^{-1}} + 2S_2^2 S_{\perp}, \end{aligned}$$

where the last line holds from Lemma 2. Finally, let \mathcal{E} be the event where $\|\Theta_{r+1:d_2,r+1:d_1}^*\|_F^2 \leq S_{\perp}$ holds, using Proposition 3 with $\delta = T^{-1}$, we know that $\mathbb{P}(\mathcal{E}^c) \leq T^{-1}$. Moreover we know that $\mathbb{P}(\mathcal{E}_t^c) \leq t^{-2}$ from Lemma 1. Therefore, we can bound the overall regret:

$$\begin{aligned} \mathcal{R}_T &\leq R_{\max} T \cdot \mathbb{P}(\mathcal{E}^c) + \mathbb{E} \left[\sum_{t=1}^T r_t \mid \mathcal{E} \right] \cdot \mathbb{P}(\mathcal{E}) \\ &\leq R_{\max} + R_{\max} T_0 + R_{\max} \cdot \sum_{t=T_0+1}^T \left(2\alpha_t \max_{i \in S_t} \|x_{it,rtv}\|_{W_t^{-1}} + 2S_2^2 \cdot S_{\perp} \right) + \sum_{t=T_0+1}^T R_{\max} \cdot \mathbb{P}(\mathcal{E}_t^c) \\ &\leq R_{\max} \left(T_0 + 1 + 2\alpha_T \sum_{t=T_0+1}^T \max_{i \in S_t} \|x_{it,rtv}\|_{W_t^{-1}} + 2S_2^2 S_{\perp} (T - T_0) \right) + R_{\max} \sum_{t=1}^T t^{-2} \\ &\leq R_{\max} \left(T_0 + 3 + 2\alpha_T \sqrt{(T - T_0) \sum_{t=T_0+1}^T \|x_{it,rtv}\|_{W_t^{-1}}^2} + 2S_2^2 S_{\perp} (T - T_0) \right) \\ &\leq R_{\max} \left(T_0 + 3 + 2\alpha_T \sqrt{T \cdot 2k \log(T/k)} + 2S_2^2 S_{\perp} (T - T_0) \right), \end{aligned}$$

which completes the proof. In the remaining section, we provide proof of Lemma 1 and 2.

S.7.4.1 Proof of Lemma 1

Define

$$J_n(\theta_{rtv}) = \sum_{t=1}^n \sum_{i \in S_t} \left(p_t(i|x_{jt,rtv}^\top \theta_{rtv}) - p_t(i|x_{jt}^\top \theta^*) \right) x_{it,rtv}.$$

Then, if $\hat{\theta}_{n,rtv}$ is the MLE of the truncated problem,

$$Z_n = J_n(\hat{\theta}_{n,rtv}) = \sum_{t=1}^n \sum_{i \in S_t} \epsilon_{it} x_{it,rtv},$$

where $\epsilon_{it} = y_{it} - p_t(i|x_{jt}^\top \theta^*)$. Note that ϵ_{it} is σ -subgaussian with $\sigma = 1/2$. Now let $W_n = \frac{1}{nK} \sum_{t=1}^n \sum_{i \in S_t} x_{it,rtv} x_{it,rtv}^\top$. Following the proof of Lemma 2 in (Oh and Iyengar, 2021), we have :

$$\|Z_n\|_{W_n^{-1}}^2 \leq \frac{2\sigma^2}{nK} \left[k \log \left(1 + \frac{n}{k} \right) + \log \frac{1}{\delta} \right],$$

with probability at least $1 - \delta$. Also following the argument on the consistency of MLE on (Oh and Iyengar, 2021), we have

$$\|J_n(\hat{\theta}_{n,rtv}) - J_n(\theta_{rtv}^*)\|_{W_n^{-1}}^2 \geq \frac{\kappa^2}{n^2 K^2} \|\hat{\theta}_{n,rtv} - \theta_{rtv}^*\|_{W_n}.$$

However, since this is the truncated space, we do not have $J_n(\theta_{rtv}^*) = 0$. Instead,

$$J_n(\theta_{rtv}^*) = \sum_{t=1}^n \sum_{i \in S_t} \left(p_t(i|x_{jt,rtv}^\top \theta_{rtv}^*) - p_t(i|x_{jt}^\top \theta^*) \right) x_{it,rtv}.$$

Now note that $p_t(i|u_j)$ is actually the expected reward at time t given the reward $r_j = 1_{\{i=j\}}$.

Using Lemma 3, we have

$$|p_t(i|x_{jt,rtv}^\top \theta_{rtv}^*) - p_t(i|x_{jt}^\top \theta^*)| \leq \max_{i \in S_t} |x_{it,rtv}^\top \theta_{rtv}^* - x_{it}^\top \theta^*| \leq S_2^2 \cdot S_\perp.$$

Therefore,

$$\|J_n(\theta_{rtv}^*)\|_{W_n^{-1}}^2 \leq S_2^4 \cdot S_\perp^2 \left(\sum_{t=1}^n \sum_{i \in S_t} |x_{it,rtv}| \right)^\top W_n^{-1} \left(\sum_{t=1}^n \sum_{i \in S_t} |x_{it,rtv}| \right)$$

$$\leq S_2^4 \cdot S_{\perp}^2 \cdot \frac{1}{nK}.$$

Then we have:

$$\begin{aligned} \|\hat{\theta}_{n,rtv} - \theta_{rtv}^*\|_{W_n} &\leq \frac{1}{\kappa} \left(\|Z_n\|_{W_n^{-1}} + \|J_n(\theta_{rtv}^*)\|_{W_n^{-1}} \right) \\ &\leq \frac{1}{\kappa n K} \left(\sigma \sqrt{2k \log \left(1 + \frac{n}{k} \right) + 4 \log n} + S_2^2 \cdot S_{\perp} \cdot \sqrt{nK} \right) =: \alpha_n, \end{aligned}$$

by plugging in $\delta = 1/n^2$.

S.7.4.2 Proof of Lemma 2

Adapting Appendix F.1 of (Kang et al., 2022), let $S_t = \arg \max_{S'} R(\{z_{it}\}, S')$, and assume $\|\hat{\theta}_{t,rtv} - \theta_{rtv}^*\|_{W_n} \leq \alpha_t$. let $z_{it} = x_{it,rtv}^\top \hat{\theta}_{t,rtv} + \beta_{it}$ where $\beta_{it} = \alpha_t \cdot \|x_{it,rtv}\|_{W_t^{-1}} + S_2^2 \cdot S_{\perp}$. Then,

$$z_{it} - \langle X_{it}, \Theta^* \rangle = x_{it,rtv}^\top \hat{\theta}_{rtv} - x_{it,rtv}^\top \theta_{rtv}^* + x_{it,rtv}^\top \theta_{rtv}^* - \langle X_{it}, \Theta^* \rangle + \beta_{it},$$

where

$$|x_{it,rtv}^\top \hat{\theta}_{rtv} - x_{it,rtv}^\top \theta_{rtv}^*| \leq \|x_{it,rtv}\|_{W_t^{-1}} \cdot \|\hat{\theta}_{rtv} - \theta_{rtv}^*\|_{W_t} \leq \alpha_t \|x_{it,rtv}\|_{W_t^{-1}},$$

and

$$|x_{it,rtv}^\top \theta_{rtv}^* - \langle X_{it}, \Theta^* \rangle| \leq \|\hat{U}_{\perp}^\top X_{it} \hat{V}\|_F \cdot \|\hat{U}_{\perp}^\top \Theta^* \hat{V}\|_F \leq S_2^2 \cdot S_{\perp}.$$

Therefore,

$$0 \leq z_{it} - \langle X_{it}, \Theta^* \rangle \leq 2\beta_t = 2\alpha_t \|x_{it,rtv}\|_{W_t^{-1}} + 2S_2^2 \cdot S_{\perp},$$

with probability at least $1 - t^{-2}$.

S.7.5 Proof of Corollary 1

Here we prove the high probability regret bound Corollary 1. The proof directly follows from the proof of Theorem 1.

Proof. Note that $\mathbb{P}(\mathcal{E}_t^c) \leq t^{-2}$. Hence, $\mathbb{P}(\cup_{t=T_0+1}^T \mathcal{E}_t^c) \leq \sum_{t=T_0+1}^T t^{-2} \leq \int_{T_0}^{\infty} t^{-2} dt = T_0^{-1}$. Therefore, $\mathbb{P}(\cap_{t=T_0+1}^T \mathcal{E}_t) \geq 1 - T_0^{-1}$. Hence,

$$r_t \leq R_{\max} \cdot 2\alpha_t \max_{i \in S_t} \|x_{it,rtv}\|_{W_t^{-1}} + 2S_2^2 S_{\perp},$$

for every $t > T_0$ with probability at least $1 - T_0^{-1}$. Hence we have the high probability bound:

$$\sum_{t=1}^T r_t \leq R_{\max} \left(T_0 + 2\alpha_T \sqrt{T \cdot 2k \log(T/k)} + 2S_2^2 S_{\perp} (T - T_0) \right), \quad (\text{S7})$$

with probability at least $1 - \delta - T_0^{-1}$. Assuming $T_0 \geq 1/\delta$, the proof is complete. \square

S.7.6 Proof of Proposition 2

In this section we prove Proposition 2, the rank estimation consistency of GIC. As GIC is a sum of the loss function (negative log likelihood) and the penalty, we prove that 1) when the rank is under-estimated, the loss is larger at a constant rate compared to the true rank; 2) when the rank is over-estimated the loss decrease is much smaller than the penalty increase. Combining these two results, the GIC is minimized at the true rank, when sample size is sufficiently large.

Proof. Let \mathcal{L}_n be the negative log likelihood given as

$$\mathcal{L}_n(\Phi) = \frac{1}{n} \sum_{t=1}^n \left[\sum_{i \in S_t} y_{it} p_i^\top \Phi q_t - \log \left(1 + \sum_{j \in S_t} \exp(p_j^\top \Phi q_t) \right) \right],$$

and let Φ_r be the rank- r constrained MLE given as

$$\hat{\Phi}_r := \arg \min_{\text{rk}(\Phi) \leq r} \mathcal{L}_n(\Phi).$$

Denote $d = \min\{d_1, d_2\}$. Note that $\hat{\Phi} = \hat{\Phi}_d = \arg \min \mathcal{L}_n(\Phi)$ is the unconstrained MLE. Therefore $\nabla \mathcal{L}_n(\hat{\Phi}) = 0$. Now using Taylor expansion we have

$$\mathcal{L}_n(\Phi) - \mathcal{L}_n(\hat{\Phi}) = (\phi - \hat{\phi})^\top \nabla^2 \mathcal{L}_n(\tilde{\phi})(\phi - \hat{\phi}).$$

And also note that

$$\nabla^2 \mathcal{L}_n(\Phi) = \frac{1}{n} \sum_{t=1}^n \left(\sum_{i \in S_t} p_{it} z_{it} z_{it}^\top - \sum_{i,j \in S_t} p_{it} p_{jt} z_{it} z_{jt}^\top \right).$$

Lemma 15 (Strong Convexity and Smoothness).

$$\frac{\kappa}{n} \lambda_{\min}(V_n) \|\phi - \hat{\phi}\|^2 \leq \mathcal{L}_n(\Phi) - \mathcal{L}_n(\hat{\Phi}) \leq \frac{1}{n} \lambda_{\max}(V_n) \|\phi - \hat{\phi}\|^2,$$

or with probability at least $1 - \delta$,

$$C_1 \|\phi - \hat{\phi}\|^2 \leq \mathcal{L}_n(\Phi) - \mathcal{L}_n(\hat{\Phi}) \leq C_2 \|\phi - \hat{\phi}\|^2.$$

The strong convexity and smoothness result follows from Lemma 5 and 8.

Lemma 16 (Estimation error for overestimated rank). *For $k \geq r^*$, we have*

$$\epsilon_k^2 := \|\hat{\Phi}_k - \Phi^*\|_F^2 \leq C \cdot \frac{d_1 d_2}{n}.$$

Proof. Note that for $k \geq r^*$,

$$\mathcal{L}_n(\hat{\Phi}) \leq \mathcal{L}_n(\hat{\Phi}_k) \leq \mathcal{L}_n(\hat{\Phi}_r).$$

Therefore,

$$\begin{aligned} C_1 \|\hat{\Phi}_k - \hat{\Phi}\|_F^2 &\leq \mathcal{L}_n(\hat{\Phi}_k) - \mathcal{L}_n(\hat{\Phi}) \\ &\leq \mathcal{L}_n(\hat{\Phi}_{r^*}) - \mathcal{L}_n(\hat{\Phi}) \\ &\leq C_2 \|\hat{\Phi}_{r^*} - \hat{\Phi}\|_F^2 \\ &\leq O\left(\frac{(d_1 + d_2)r}{n}\right), \end{aligned}$$

and hence, $\|\hat{\Phi}_k - \hat{\Phi}\|_F = O\left(\sqrt{\frac{(d_1 + d_2)r}{n}}\right)$. Note that $\|\hat{\Phi} - \Phi^*\|_F^2 = O\left(\frac{d_1 d_2}{n}\right)$. Therefore, $\|\hat{\Phi}_k - \Phi^*\|_F = O\left(\sqrt{\frac{d_1 d_2}{n}}\right)$. \square

Lemma 17 (Estimation error for underestimated rank). *For $k \leq r^*$, we have*

$$\epsilon_k^2 := \|\hat{\Phi}_k - \Phi^*\|_F^2 \geq C \cdot \sum_{i=k+1}^{r^*} \sigma_i^2.$$

Then for $r < r^*$, we have:

$$\begin{aligned} \mathcal{L}_n(\hat{\Phi}_r) - \mathcal{L}_n(\hat{\Phi}_{r^*}) &= (\mathcal{L}_n(\hat{\Phi}_r) - \mathcal{L}_n(\hat{\Phi})) - (\mathcal{L}_n(\hat{\Phi}_{r^*}) - \mathcal{L}_n(\hat{\Phi})) \\ &\geq C_1 \|\hat{\phi}_r - \hat{\phi}\|^2 \\ &\geq C_1 (\epsilon_r - \epsilon_d)^2 \\ &\rightarrow C_1 \epsilon_r^2. \end{aligned}$$

Similarly, for $r > r^*$, we have:

$$\begin{aligned} \mathcal{L}_n(\hat{\Phi}_r) - \mathcal{L}_n(\hat{\Phi}_{r^*}) &= (\mathcal{L}_n(\hat{\Phi}_r) - \mathcal{L}_n(\hat{\Phi})) - (\mathcal{L}_n(\hat{\Phi}_{r^*}) - \mathcal{L}_n(\hat{\Phi})) \\ &\geq C_1 \|\hat{\phi}_r - \hat{\phi}\|^2 - C_2 \|\hat{\phi}_{r^*} - \hat{\phi}\|^2 \\ &\geq C_1 (\epsilon_r - \epsilon_d)^2 - C_2 (\epsilon_{r^*} + \epsilon_d)^2. \end{aligned}$$

and therefore, $\mathcal{L}_n(\hat{\Phi}_{r^*}) - \mathcal{L}_n(\hat{\Phi}_r) = O(\epsilon_d^2) = O(\frac{d_1 d_2}{n})$.

Now define the penalty $P(r)$ as

$$P(r) = a_n \cdot (d_1 + d_2 - r) \cdot r.$$

Then,

$$P(r) - P(r^*) = a_n (d_1 + d_2 - r - r^*) (r - r^*).$$

Note that GIC will be defined as

$$GIC(r) := \mathcal{L}_n(\hat{\Phi}_r) + P(r).$$

If we define $a_n = \log(n)/n$, $GIC(r) > GIC(r^*)$ as $n \rightarrow \infty$ for $r \neq r^*$. \square

References

Abbasi-Yadkori, Y., Pal, D., and Szepesvari, C. (2012). Online-to-confidence-set conversions and application to sparse stochastic bandits. In *Artificial Intelligence and Statistics*, pages 1–9. PMLR.

Adam, Hamner, B., Friedman, D., and SSA_Expedia (2013). Personalize expedia hotel searches - ICDM 2013. Kaggle. <https://kaggle.com/competitions/expedia-personalized-sort>.

Agrawal, S., Avadhanula, V., Goyal, V., and Zeevi, A. (2017). Thompson sampling for the MNL-bandit. In *Conference on Learning Theory*, pages 76–78. PMLR.

Agrawal, S., Avadhanula, V., Goyal, V., and Zeevi, A. (2019). Mnl-bandit: A dynamic learning approach to assortment selection. *Operations Research*, 67(5):1453–1485.

Akaike, H. (1987). Factor analysis and aic. *Psychometrika*, 52:317–332.

Aouad, A., Feldman, J., and Segev, D. (2023). The exponomial choice model for assortment optimization: an alternative to the MNL model? *Management Science*, 69(5):2814–2832.

Auer, P. (2002). Using confidence bounds for exploitation-exploration trade-offs. *Journal of Machine Learning Research*, 3(Nov):397–422.

Bell, R. M. and Koren, Y. (2007). Lessons from the netflix prize challenge. *Acm Sigkdd Explorations Newsletter*, 9(2):75–79.

Bobadilla, J., Ortega, F., Hernando, A., and Gutiérrez, A. (2013). Recommender systems survey. *Knowledge-Based Systems*, 46:109–132.

Burer, S. and Monteiro, R. D. (2003). A nonlinear programming algorithm for solving semidefinite programs via low-rank factorization. *Mathematical Programming*, 95(2):329–357.

Cai, J., Chen, R., Wainwright, M. J., and Zhao, L. (2023). Doubly high-dimensional contextual bandits: An interpretable model for joint assortment-pricing. *arXiv preprint arXiv:2309.08634*.

Caro, F. and Gallien, J. (2007). Dynamic assortment with demand learning for seasonal consumer goods. *Management Science*, 53(2):276–292.

Chakraborty, B. and Murphy, S. A. (2014). Dynamic treatment regimes. *Annual Review of Statistics and Its Application*, 1:447–464.

Chen, X., Krishnamurthy, A., and Wang, Y. (2023). Robust dynamic assortment optimization in the presence of outlier customers. *Operations Research*, 72(3):999–1015.

Chen, X. and Wang, Y. (2018). A note on a tight lower bound for capacitated mnl-bandit assortment selection models. *Operations Research Letters*, 46(5):534–537.

Chen, X., Wang, Y., and Zhou, Y. (2020). Dynamic assortment optimization with changing contextual information. *The Journal of Machine Learning Research*, 21(1):8918–8961.

Cheung, W. C. and Simchi-Levi, D. (2017). Thompson sampling for online personalized assortment optimization problems with multinomial logit choice models. *Available at SSRN 3075658*.

Chi, Y., Lu, Y. M., and Chen, Y. (2019). Nonconvex optimization meets low-rank matrix factorization: An overview. *IEEE Transactions on Signal Processing*, 67(20):5239–5269.

Dai, B., Shen, X., Wang, J., and Qu, A. (2021). Scalable collaborative ranking for personalized prediction. *Journal of the American Statistical Association*, 116(535):1215–1223.

Dai, B., Wang, J., Shen, X., and Qu, A. (2019). Smooth neighborhood recommender systems. *Journal of Machine Learning Research*, 20(16):1–24.

Fan, Y. and Tang, C. Y. (2013). Tuning parameter selection in high dimensional penalized likelihood. *Journal of the Royal Statistical Society Series B: Statistical Methodology*, 75(3):531–552.

Goyal, V. and Perivier, N. (2022). Dynamic pricing and assortment under a contextual mnl demand. *Advances in Neural Information Processing Systems*, 35:3461–3474.

Ibriga, H. S. and Sun, W. W. (2023). Covariate-assisted sparse tensor completion. *Journal of the American Statistical Association*, 118(544):2605–2619.

Jain, P., Netrapalli, P., and Sanghavi, S. (2013). Low-rank matrix completion using alternating minimization. In *Proceedings of the forty-fifth annual ACM symposium on Theory of Computing*, pages 665–674.

Javanmard, A., Nazerzadeh, H., and Shao, S. (2020). Multi-product dynamic pricing in high-dimensions with heterogeneous price sensitivity. In *2020 IEEE International Symposium on Information Theory (ISIT)*, pages 2652–2657. IEEE.

Jun, K.-S., Willett, R., Wright, S., and Nowak, R. (2019). Bilinear bandits with low-rank structure. In *International Conference on Machine Learning*, pages 3163–3172. PMLR.

Kallus, N. and Udell, M. (2020). Dynamic assortment personalization in high dimensions. *Operations Research*, 68(4):1020–1037.

Kang, Y., Hsieh, C.-J., and Lee, T. C. M. (2022). Efficient frameworks for generalized low-rank matrix bandit problems. *Advances in Neural Information Processing Systems*, 35:19971–19983.

Kim, G.-S. and Paik, M. C. (2019). Doubly-robust lasso bandit. *Advances in Neural Information Processing Systems*, 32:5877–5887.

Konishi, S. and Kitagawa, G. (1996). Generalised information criteria in model selection. *Biometrika*, 83(4):875–890.

Koren, Y., Bell, R., and Volinsky, C. (2009). Matrix factorization techniques for recommender systems. *Computer*, 42(8):30–37.

Kveton, B., Szepesvári, C., Rao, A., Wen, Z., Abbasi-Yadkori, Y., and Muthukrishnan, S. (2017). Stochastic low-rank bandits. *arXiv preprint arXiv:1712.04644*.

Lattimore, T. and Szepesvári, C. (2020). *Bandit algorithms*. Cambridge University Press.

Li, L., Lu, Y., and Zhou, D. (2017). Provably optimal algorithms for generalized linear contextual bandits. In *International Conference on Machine Learning*, pages 2071–2080. PMLR.

Lika, B., Kolomvatsos, K., and Hadjiefthymiades, S. (2014). Facing the cold start problem in recommender systems. *Expert systems with applications*, 41(4):2065–2073.

Liu, D. C. and Nocedal, J. (1989). On the limited memory BFGS method for large scale optimization. *Mathematical Programming*, 45(1):503–528.

Luo, Y., Sun, W. W., and Liu, Y. (2024). Distribution-free contextual dynamic pricing. *Mathematics of Operations Research*, 49(1):599–618.

Ma, S., Niu, P.-Y., Zhang, Y., and Zhu, Y. (2024). Statistical inference for noisy matrix completion incorporating auxiliary information. *Journal of the American Statistical Association*, (just-accepted):1–24.

Mao, X., Chen, S. X., and Wong, R. K. (2019). Matrix completion with covariate information. *Journal of the American Statistical Association*, 114(525):198–210.

McFadden, D. (1974). Conditional logit analysis of qualitative choice behavior. *Frontiers in Econometrics*, pages 105–142.

Morimoto, T., Hung, H., and Huang, S.-Y. (2024). Information criterion-based rank estimation methods for factor analysis: A unified selection consistency theorem and numerical comparison. *arXiv preprint arXiv:2407.19959*.

Oh, M.-h. and Iyengar, G. (2021). Multinomial logit contextual bandits: Provable optimality and practicality. In *Proceedings of the AAAI Conference on Artificial Intelligence*, volume 35, pages 9205–9213.

Park, S., Lee, E. R., and Zhao, H. (2024). Low-rank regression models for multiple binary responses and their applications to cancer cell-line encyclopedia data. *Journal of the American Statistical Association*, 119(545):202–216.

Robin, G., Wai, H.-T., Josse, J., Klopp, O., and Moulines, É. (2018). Low-rank interaction with sparse additive effects model for large data frames. *Advances in Neural Information Processing Systems*, 31.

Rusmevichtong, P., Shen, Z.-J. M., and Shmoys, D. B. (2010). Dynamic assortment optimization with a multinomial logit choice model and capacity constraint. *Operations Research*, 58(6):1666–1680.

Sarwar, B., Karypis, G., Konstan, J., and Riedl, J. T. (2000). Application of dimensionality reduction in recommender system-a case study. *Proceedings of the ACM WebKDD, 2000*.

Sauré, D. and Zeevi, A. (2013). Optimal dynamic assortment planning with demand learning. *Manufacturing & Service Operations Management*, 15(3):387–404.

Schein, A. I., Popescul, A., Ungar, L. H., and Pennock, D. M. (2002). Methods and metrics for cold-start recommendations. In *Proceedings of the 25th annual international ACM SIGIR conference on Research and development in information retrieval*, pages 253–260.

Shao, J., Dong, R., and Zheng, Z. (2022). Sparse assortment personalization in high dimensions. *JUSTC*, 52(3):5.

Shi, C., Fan, A., Song, R., and Lu, W. (2018). High-dimensional a-learning for optimal dynamic treatment regimes. *Annals of Statistics*, 46(3):925–957.

Shi, C., Wan, R., Song, G., Luo, S., Zhu, H., and Song, R. (2023). A multiagent reinforcement learning framework for off-policy evaluation in two-sided markets. *The Annals of Applied Statistics*, 17(4):2701–2722.

Sumida, M. and Zhou, A. (2023). Optimizing and learning assortment decisions in the presence of platform disengagement. *Available at SSRN 4537925*.

Tropp, J. A. (2012). User-friendly tail bounds for sums of random matrices. *Foundations of Computational Mathematics*, 12:389–434.

Udell, M. and Townsend, A. (2019). Why are big data matrices approximately low rank? *SIAM Journal on Mathematics of Data Science*, 1(1):144–160.

Van der Vaart, A. W. (2000). *Asymptotic statistics*, volume 3. Cambridge university press.

Van Meteren, R. and Van Someren, M. (2000). Using content-based filtering for recommendation. In *Proceedings of the Machine Learning in the New Information Age: MLnet/ECML2000 workshop*, volume 30, pages 47–56. Barcelona.

Vershynin, R. (2010). Introduction to the non-asymptotic analysis of random matrices. *arXiv preprint arXiv:1011.3027*.

Wainwright, M. J. (2019). *High-dimensional statistics: A non-asymptotic viewpoint*, volume 48. Cambridge university press.

Wang, L., Zhang, X., and Gu, Q. (2017). A unified computational and statistical framework for nonconvex low-rank matrix estimation. In *Artificial Intelligence and Statistics*, pages 981–990. PMLR.

Wang, X., Wei, M. M., and Yao, T. (2019). Online assortment optimization with high-dimensional data. *Available at SSRN 3521843*.

Xia, D. and Yuan, M. (2021). Statistical inferences of linear forms for noisy matrix completion. *Journal of the Royal Statistical Society Series B: Statistical Methodology*, 83(1):58–77.

Xia, D., Zhang, A. R., and Zhou, Y. (2022). Inference for low-rank tensors—no need to debias. *The Annals of Statistics*, 50(2):1220–1245.

Xu, Y. and Wang, Z. (2023). Assortment optimization for a multistage choice model. *Manufacturing & Service Operations Management*, 25(5):1748–1764.

Zhang, J., Sun, W. W., and Li, L. (2023). Generalized connectivity matrix response regression with applications in brain connectivity studies. *Journal of Computational and Graphical Statistics*, 32(1):252–262.

Zhao, Y.-Q., Zeng, D., Laber, E. B., and Kosorok, M. R. (2015). New statistical learning methods for estimating optimal dynamic treatment regimes. *Journal of the American Statistical Association*, 110(510):583–598.

Zhen, Y. and Wang, J. (2024). Nonnegative tensor completion for dynamic counterfactual prediction on covid-19 pandemic. *The Annals of Applied Statistics*, 18(1):224–245.

Zheng, Q. and Lafferty, J. (2016). Convergence analysis for rectangular matrix completion using burer-monteiro factorization and gradient descent. *arXiv preprint arXiv:1605.07051*.

Zhou, J., Hao, B., Wen, Z., Zhang, J., and Sun, W. W. (2024a). Stochastic low-rank tensor bandits for multi-dimensional online decision making. *Journal of the American Statistical Association*, (just-accepted):1–25.

Zhou, W., Zhu, R., and Qu, A. (2024b). Estimating optimal infinite horizon dynamic treatment regimes via pt-learning. *Journal of the American Statistical Association*, 119(545):625–638.